2008

Approximating The Spectral Width Of Irradiance Fluctuations With Quasi-frequency

Andrew Reel
University of Central Florida

APPROXIMATING THE SPECTRAL WIDTH OF IRRADIANCE FLUCTUATIONS WITH QUASI-FREQUENCY

by

ANDREW STEVEN REEL
B.A. University of Central Florida, 1998

A thesis submitted in partial fulfillment of the requirements
for the degree of Master of Science
in the Department of Mathematics
in the College Sciences
at the University of Central Florida
Orlando, Florida

Spring Term
2008

ABSTRACT

Under weak turbulence theory, we will use the random thin phase screen model and the Kolmogorov power-law spectrum to derive approximate models for the scintillation index, covariance function of irradiance fluctuations, and temporal spectrum of irradiance fluctuations for collimated beams. In addition, we will provide an expression for the quasi-frequency of a collimated beam and investigate the relationship between the quasi-frequency and the maximum width of the normalized temporal spectrum of irradiance for a collimated beam.

ACKNOWLEDGMENTS

I want to thank God for His guidance in my life. I want to thank my wife and family for their support. Finally, I want to thank Dr. Larry Andrews for his patience, time, wisdom, and guidance throughout this project.

TABLE OF CONTENTS

LIST OF FIGURES

INTRODUCTION

Movement of light through a dynamic medium can create a variety of effects that most people have observed throughout history. For example, stars in the night sky may appear to twinkle or while driving down a long straight road during the middle of the day, a hazy layer of movement may appear above the road's surface. The earth's atmosphere is a continuously changing medium that affects the way we perceive light and images. If we study a laser beam propagating through the earth's atmosphere, we find that the beam collected at a receiver may vary in intensity and/or may continuously be changing its position.

While studying laser propagation through a random medium, statistical models are used to describe propagation environments and beam characteristics. To describe the turbulent nature of the earth's atmosphere, where each point in space and time can be represented by a random variable, we commonly use a stochastic field. By using a stochastic field to model atmospheric turbulence, we can use statistical tools to investigate beam characteristics. One of the most important beam characteristics is the intensity, or irradiance, of the laser at a receiver. Propagating a beam through a continuously changing medium can cause fluctuations in a laser's irradiance; these fluctuations are often referred to as "scintillation." The scintillation index is a phrase used to describe the normalized irradiance fluctuations at a single point on a receiver. Another useful beam characteristic, closely related to the scintillation index, is called the covariance function of irradiance fluctuations. A covariance function is used to describe the correlation of irradiance fluctuations between two separate points on a receiver. The scintillation index and covariance function are considered spatial functions because of their dependence on

points within the beam. Since a stochastic field also treats time as a variable, we can use the frozen turbulence hypothesis to express the covariance function in terms of the temporal domain and then we can calculate the temporal spectrum of irradiance fluctuations. The frozen turbulence hypothesis assumes that turbulent eddies are frozen in shape and move by the receiver with average transverse wind speed. Hence, spatial separations can be converted to the temporal domain by including the wind speed. Moreover, through the use of a phase screen model, we will be able to derive approximate expressions for the scintillation index, the covariance function and temporal spectrum of irradiance fluctuations. Once we have an expression for the temporal spectrum, we can normalize it to create a function that has characteristics like a probability density function. By treating the normalized spectrum as a probability density function, we can further describe beam characteristics and look for any relations through standard statistical tools.

BACKGROUND

Optical Wave Models

Lasers are devices that produce coherent radiation in wavelengths typically ranging from the infrared to the ultraviolet regions of the electromagnetic spectrum. From Figure 1, we see that some lasers produce radiation with wavelengths in the range of visible light. A laser beam is commonly referred to as an optical beam.

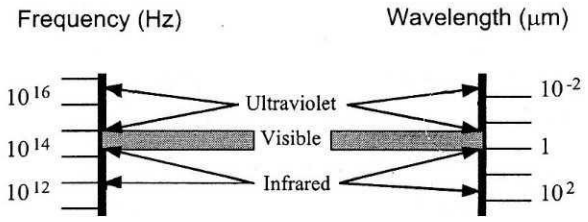

Figure 1: A portion of the electromagnetic spectrum.

There are three optical wave models that are commonly used to study laser propagation, assuming propagation is along the positive z-axis. The first model is the plane wave, which is described by an unbounded wave with constant amplitude A_0, constant phase φ_0, and in the plane of the transmitter ($z = 0$) it is represented by

$$U_0(x, y, 0) = A_0 e^{i\varphi_0}, \qquad 1$$

The next is the spherical wave model, which is described by an unbounded wave associated with a point source and in the plane of the transmitter ($z = 0$) it is represented by

$$U_0(x,y,0) = \lim_{R\to 0} \frac{e^{ikR}}{4\pi R}, \qquad 2$$

where $R = \left|\vec{R}\right| = \sqrt{x^2 + y^2 + z^2}$. Finally, the beam or Gaussian-beam model describes a wave of finite size with focusing capabilities. It has amplitude and phase profile described in the plane of the transmitter ($z = 0$) by

$$U_0(x,y,0) = a_0 \exp\left[-\frac{x^2 + y^2}{W_0^2} - \frac{ik}{2F_0}\left(x^2 + y^2\right)\right], \qquad 3$$

where a_0 is the on-axis amplitude, W_0 is the beam spot radius, and F_0 is its phase front radius of curvature at the transmitter. Of the three models, the Gaussian-beam model will be used throughout this paper.

Propagation Of Gaussian-Beam Waves Through Free-Space

Studying a beam propagating through free-space, an environment devoid of turbulence, allows us to describe characteristics and define important parameters of the beam at both the transmitter and receiver, see Figure 2. At the transmitter or input plane ($z = 0$), we have the following beam characteristics;

Wave number: $k = \frac{2\pi}{\lambda}$, where λ is the wavelength

Spot size radius: W_0

Phase front radius of curvature: F_0.

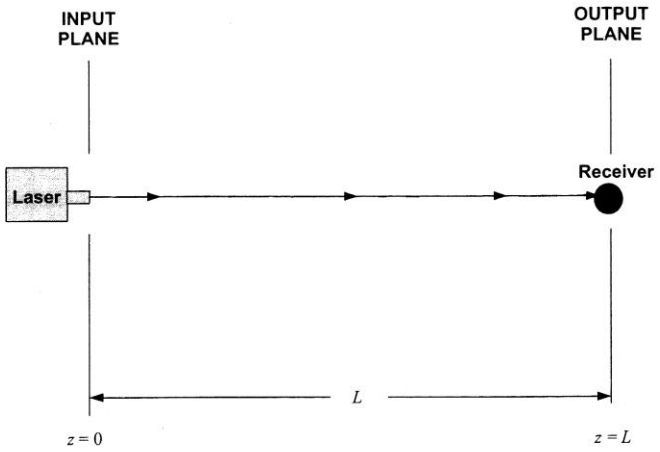

Figure 2: Laser propagating through free space.

By using the above characteristics, we can define a set of input plane beam parameters with z representing the propagation length as

$$\Theta_0 = 1 - \frac{z}{F_0} \qquad \text{and} \qquad \Lambda_0 = \frac{2z}{kW_0^2}. \tag{4}$$

Note that Θ_0 and Λ_0 are dimensionless quantities. As for the receiver or output plane ($z = L$), we can define a set of output plane beam parameters in terms of the input plane parameters as

$$\Theta = \frac{\Theta_0}{\Theta_0^2 + \Lambda_0^2} = 1 + \frac{z}{F} \qquad \text{and} \qquad \Lambda = \frac{\Lambda_0}{\Theta_0^2 + \Lambda_0^2} = \frac{2z}{kW^2}, \tag{5}$$

where F is the phase front radius of curvature at the receiver and W is the spot size at the receiver. A third output plane parameter is commonly used to simplify many expressions in propagation analysis; it is called the complementary parameter and is defined as

$$\overline{\Theta} = 1 - \Theta. \tag{6}$$

Medium Models

As the earth rotates, its surface continuously goes through a cycle of heating and cooling, which creates a combination of temperature and wind speed variations. L. F. Richardson [1] developed the energy cascade theory, which illustrates how transformation of energy, originating from the sun, creates unstable air masses (or eddies) throughout the earth's atmosphere. As energy is transferred, large eddies are broken into smaller ones until the energy is dissipated as heat, see Figure 3. The size of the large eddies will be denoted as L_0 and are referred to as the outer scale of turbulence. As for the size of the smaller eddies, they will be denoted as l_0 and are referred to as the inner scale of turbulence.

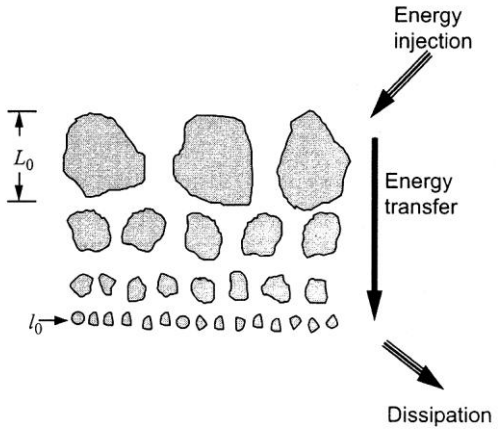

Figure 3: Visualization of the energy cascade theory.

Figure 4 illustrates an optical wave propagating from a transmitter to a receiver through a medium consisting of various sized eddies. Studies have shown that eddies act like lenses that change the beam's direction and/or focal point. The propagation environment illustrated in Figure 4 is called an extended medium model, where the random medium exists everywhere

between the transmitter and receiver. Most propagation environments, when propagating over a horizontal path, are of the extended medium model.

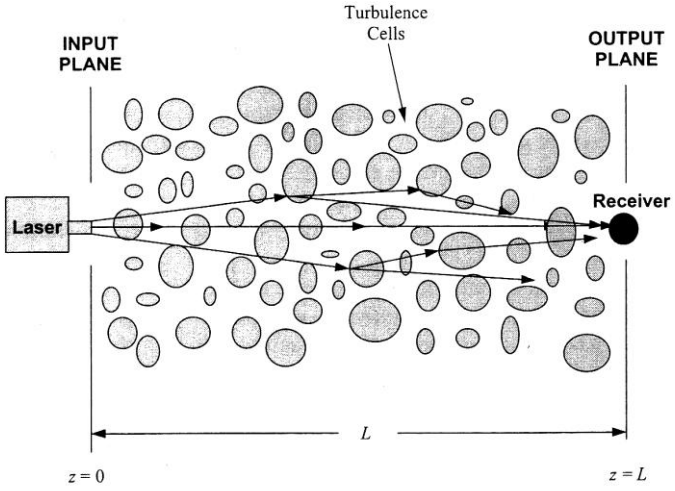

Figure 4: Extended medium model.

Figure 5 shows a propagation environment where the random medium does not exist everywhere between the transmitter and receiver, but is restricted to a thin layer. The environment illustrated in Figure 5 is called a thin random phase screen model and we will find later that using this model will allow us to simplify certain conditions which will lead to the easier evaluation of some integrals. Note that many of the calculations in this paper are done using the random phase screen model as an approximation to the extended turbulence model.

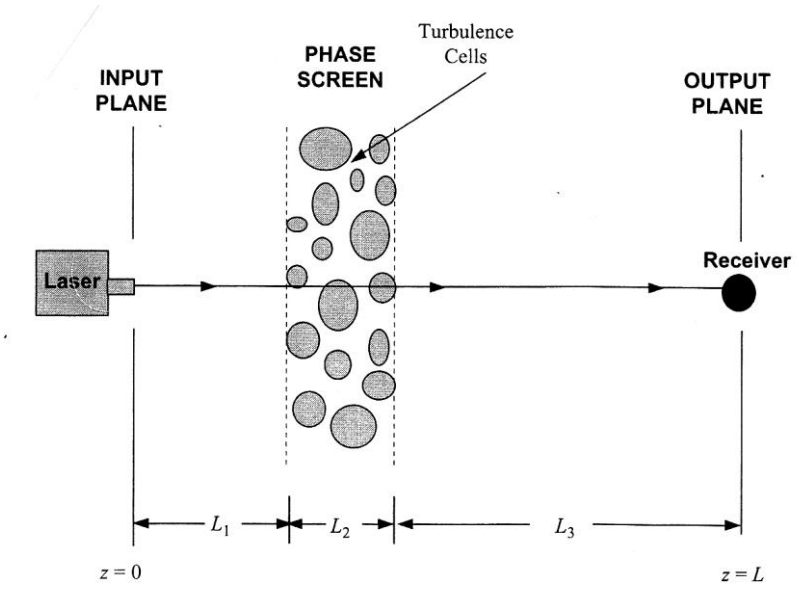

Figure 5: Phase screen model.

Refractive Index Fluctuations

Suppose a beam of light intercepts, but not perpendicular to, a plane of glass. Experiments have shown that part of the incident light is reflected by the surface of the glass, while the rest is refracted, meaning that some of the incident light passes through the surface and into the glass, see Figure 6. [2]

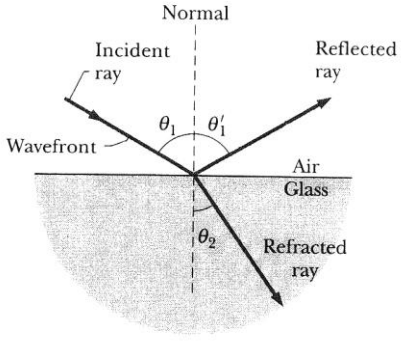

Figure 6: Refractive and reflected light from light intersecting with a plane of glass.

The term index of refraction is used to describe the amount of refractive effect on light propagating through a particular medium. When studying beam propagation, index of refraction is an important dimensionless parameter of the atmosphere. Studies have shown the refractive index to be very sensitive to small fluctuations in temperature while fluctuations in pressure and humidity are usually neglected. In addition, the index of refraction encountered by light in any medium besides vacuum space depends on the wave number (wavelength) of the light.

Due to its random nature, the atmosphere is treated as a stochastic field, where each point in space and time can be represented as a random variable. When a random field is statistically homogeneous and isotropic, it means that statistical moments are invariant under a spatial translation and rotation, respectively. By assuming the atmosphere is statistically homogeneous and isotropic, we are led to simpler power spectrum models for refractive index fluctuations. A well-known and commonly used model is called the *Kolmogorov power-law spectrum* and is defined by

$$\Phi_n(\kappa) = 0.033 C_n^2 \kappa^{-11/3}, \text{ for } 1/L_0 << \kappa << 1/l_0 . \qquad 7$$

In the Kolmogorov spectrum, κ is the scalar spatial frequency (with units of rad/m) and C_n^2 is called the index of refraction structure constant (with units of $m^{-2/3}$). Although other spectrum models have been developed for dealing with the effects of the outer and inner scales of turbulence, denoted by L_0 and l_0, respectively. All calculations throughout this paper have been completed using the Kolmogorov spectrum.

Fluctuations in the refractive index lead to a number of detrimental effects on an optical wave. One such effect is the fluctuation of intensity or irradiance of the optical wave at a

receiver. The term scintillation or scintillation index is used to describe fluctuations in the received irradiance resulting from propagating through atmospheric turbulence. Studies in optical wave propagation use scintillation to classify atmospheric conditions in terms of either weak or strong fluctuations. It is customary to use the Rytov variance, defined as

$$\sigma_R^2 = 1.23 C_n^2 k^{7/6} L^{11/6}, \qquad 8$$

to distinguish between weak and strong fluctuation conditions. In the case of a Gaussian-beam, weak fluctuations are characterized by the set of conditions where

$$\sigma_R^2 < 1 \qquad \text{and} \qquad \sigma_R^2 \Lambda^{5/6} < 1.$$

RANDOM PHASE SCREEN MODEL

As stated earlier, propagating environments over horizontal paths are primary described by the extended medium model, see Figure 2, where the random medium extends from the transmitter ($z = 0$) to the receiver ($z = L$). Random phase screens are turbulent layers that lay in the propagation path; some examples could be scattering from a rough sea surface or smoke and heat caused from a fire. Both cases describe an extended medium environment with a random phase screen somewhere in the path of propagation. Booker el at [3] made a comparative study between the extended medium and phase screen models. Later, Andrews el al [4] extended the phase screen analysis to the Gaussian-beam wave, where the model is described as a turbulent layer arbitrarily located between the transmitter and the receiver in a free space environment, see Figure 7. Using Andrews' model, let's assume the path of propagation is along the *z*-axis with the transmitter positioned at $z = 0$ and the receiver positioned at $z = L$. In addition, let's assume the random layer exists only between the planes $z = L_1$ and $z = L_1 + L_2$. Observe that the path of propagation is $L = L_1 + L_2 + L_3$. Andrews has shown that using the random phase screen model can simplify the mathematics associated with statistical models of optical wave propagation by taking the turbulent layer to be very "thin." [5] By "thin" layer, we mean that the length of L_2 is much smaller than the length L_3 or it is common to say $\frac{L_2}{L_3} << 1$. Many of the statistical models require integrating expressions over the path of propagation; integrating with respect to *z* from 0 to *L*.

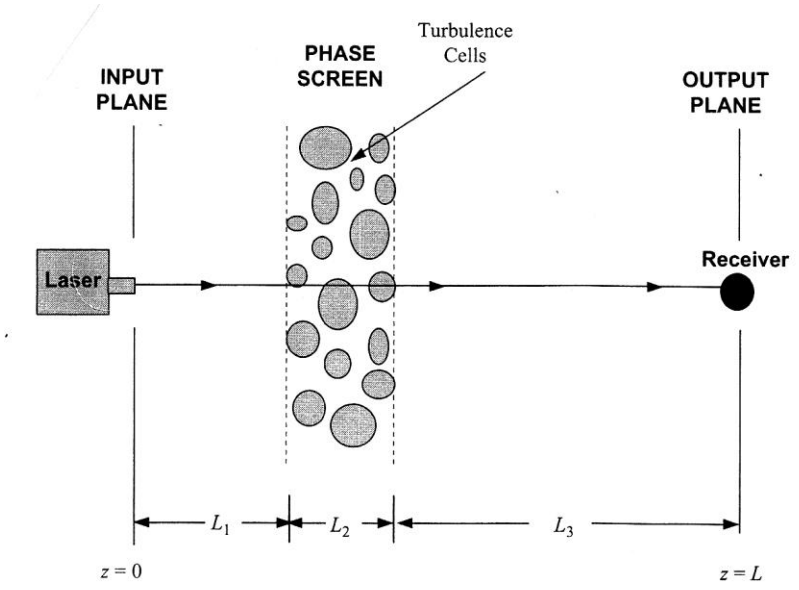

Figure 7: Phase screen model.

Let $\Phi_n(\kappa)$ represent the power spectrum for refractive index fluctuations of the turbulent layer. Since L_1 and L_3 are the regions of free space and the power spectrum applies only to the interval $L_1 \le z \le L_1 + L_2$, then

$$\Phi_n(\kappa) = \begin{cases} 0 \;; & 0 \le z \le L_1 \\ 0.033\hat{C}_n^2 \kappa^{-11/3} \;; & L_1 \le z \le L_1 + L_2 \\ 0 \;; & L_1 + L_2 \le z \le L \end{cases}.$$

Hence, using a thin random phase screen model allows for integration over a smaller interval. Normalizing the propagation path, $1 - \frac{z}{L}$, often simplifies the integration process. Under the thin phase screen model, normalizing the interval of contribution, $L_1 \le z \le L_1 + L_2$ allows for further simplifications. Let's define $d_2 = \frac{L_2}{L_3}$, and $d_3 = \frac{L_3}{L}$, so that

$$1-\frac{z}{L}=d_3\left(1+d_2\eta\right) \qquad 9$$

where $0\le\eta\le 1$. Observe that when $\eta=0$, then $z=L_1+L_2$ and when $\eta=1$, then $z=L_1$, see Figure 8. In addition, note that $Ld_2d_3=L\left(\frac{L_2}{L_3}\right)\left(\frac{L_3}{L}\right)=L_2$.

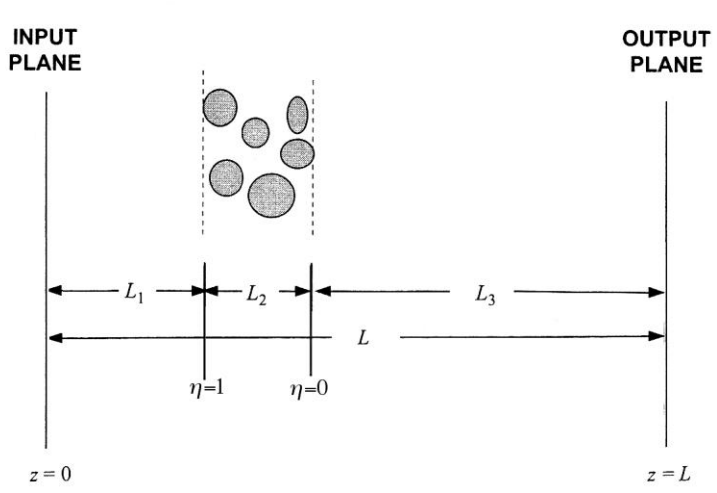

Figure 8: Phase screen model with a change of variable of integration from *L* to η.

Rather than integrate with respect to *z*, the variable of integration would become η. Making a change of variable of integration from *z* to η, we have

$$\int_0^L dz=\int_{L_1}^{L_1+L_2} dz \Rightarrow \int_1^0 -L_2\,d\eta=L_2\int_0^1 d\eta \,.$$

Making the assumption of a thin phase screen implies that $d_2 = \frac{L_2}{L_3} << 1$ and since $0 \le \eta \le 1$, then (9) simplifies to $d_3(1 + d_2\eta) \cong d_3$. Hence, using the thin phase screen model, described by Andrews, [5] allows for approximations to be made which eliminate the requirement to integrate over the propagation path. In addition, Andrews has shown the Rytov variance for a thin random phase screen model to be

$$\hat{\sigma}_R^2 = 2.25\hat{C}_n^2 k^{7/6} L^{11/6} d_2 d_3^{11/6}, \qquad 10$$

where $\hat{C}_n^2$ is the refractive structure constant of the phase screen. Enforcing equivalence between (8) and (10) leads to the relation between the refractive structure constants of the extended medium and phase screen models to be

$$C_n^2 = 1.83 d_2 d_3^{11/6} \hat{C}_n^2 = 1.83 d_3^{11/6} \frac{L_2}{L} \hat{C}_n^2.$$

SCINTILLATION INDEX

The analysis that follows is completed under the following assumptions; weak optical turbulence theory and turbulence is statistically homogeneous and isotropic. By studying fourth-order statistical moments of the optical field, we can derive expressions for irradiance fluctuations. Using the extended medium model, it has been shown that the scintillation index, which describes irradiance fluctuations at a single point in the receiver plane, can be approximated by [5]

$$\sigma_I^2(\vec{r},L)=8\pi^2k^2L\int_0^1\int_0^\infty \kappa\Phi_n(\kappa)\exp\left(-\frac{\Lambda L\kappa^2\xi^2}{k}\right)\left\{I_0(2\Lambda r\kappa\xi)-\cos\left[\frac{L\kappa^2}{k}\xi\left(1-\overline{\Theta}\xi\right)\right]\right\}d\kappa d\xi, \qquad 11$$

where $I_0(x)$ is a modified Bessel function of the first kind, see A17 in appendix A, κ is the scalar spatial frequency, $\Phi_n(\kappa)$ is the power spectrum model, $\vec{r}$ describes a vector in the transverse plane at $z = L$, $r=|\vec{r}|$, Λ and $\overline{\Theta}$ are beam parameters, and ξ represents the normalized distance variable defined as

$$\xi=1-\frac{z}{L}. \qquad 12$$

It is often convenient to express the scintillation index as a sum of two integrals that are interpreted as the radial and longitudinal components of the scintillation index and are identified respectively as

$$\sigma_{I,r}^2(\vec{r},L)=8\pi^2k^2L\int_0^1\int_0^\infty \kappa\Phi_n(\kappa)\exp\left(-\frac{\Lambda L\kappa^2\xi^2}{k}\right)\left\{I_0(2\Lambda r\xi\kappa)-1\right\}d\kappa d\xi, \tag{13}$$

and

$$\sigma_{I,l}^2(\vec{r},L)=8\pi^2k^2L\int_0^1\int_0^\infty \kappa\Phi_n(\kappa)\exp\left(-\frac{\Lambda L\kappa^2\xi^2}{k}\right)\left\{1-\cos\left[\frac{L\kappa^2}{k}\xi\left(1-\overline{\Theta}\xi\right)\right]\right\}d\kappa d\xi. \tag{14}$$

It has been shown that after completing the integrals, the radial and longitudinal components become

$$\sigma_{I,r}^2(\vec{r},L)=2.64\sigma_R^2\Lambda^{5/6}\left[1-{}_1F_1\left(-\frac{5}{6};1;\frac{2r^2}{W^2}\right)\right], \tag{15}$$

and

$$\sigma_{I,l}^2(\vec{r},L)=3.86\sigma_R^2\,\mathrm{Re}\left[i^{5/6}{}_2F_1\left(-\frac{5}{6},\frac{11}{6};\frac{17}{6};\overline{\Theta}+i\Lambda\right)-\frac{11}{16}\Lambda^{5/6}\right], \tag{16}$$

or as the total scintillation

$$\sigma_I^2(\vec{r},L)=3.86\sigma_R^2\,\mathrm{Re}\left[i^{5/6}{}_2F_1\left(-\frac{5}{6},\frac{11}{6};\frac{17}{6};\overline{\Theta}+i\Lambda\right)\right]-2.64\sigma_R^2\Lambda^{5/6}{}_1F_1\left(-\frac{5}{6};1;\frac{2r^2}{W^2}\right), \tag{17}$$

where ${}_pF_q(z)$ denotes a generalized hypergeometric function, see A16 in appendix A.

Typically, it is useful to have simple and accurate approximations for the scintillation index. Using the small argument asymptotic form (A13) of the radial component and forming an

approximation of the longitudinal component in the case of a collimated beam, the total scintillation index becomes

$$\sigma_I^2(r,L) \cong 4.42\sigma_R^2\Lambda^{5/6}\frac{r^2}{W^2} + 3.86\sigma_R^2\left\{0.40\left[(1+2\Theta)^2 4\Lambda^2\right]^{5/12}\cos\left[\frac{5}{6}\tan^{-1}\left(\frac{1+2\Theta}{2\Lambda}\right)\right] - \frac{11}{16}\Lambda^{5/6}\right\},$$

where $r < W$. 18

Let's use Andrews' thin phase screen model, in which the turbulent medium is confined within a thin layer and use the Kolmogorov power-law spectrum, $\Phi_n(\kappa) = 0.033\hat{C}_n^2\kappa^{-11/3}$, to evaluate (11). Additionally, let's assume the random medium exits along the propagation path only over the interval $L_1 \le z \le L_1 + L_2$, see Figures 7 or 8. Thus the Kolmogorov power-law spectrum applies only to the interval $L_1 \le z \le L_1 + L_2$, giving

$$\Phi_n(\kappa) = \begin{cases} 0 \ ; & 0 \le z \le L_1 \\ 0.033\hat{C}_n^2\kappa^{-11/3} \ ; & L_1 \le z \le L_1 + L_2 \\ 0 \ ; & L_1 + L_2 \le z \le L \end{cases}. \quad 19$$

Just as ξ, defined by (12), was used to represent the normalized distance in (11), let's introduce a new normalized distance variable for the interval $L_1 \le z \le L_1 + L_2$. Let's take

$$1 - \frac{z}{L} = d_3(1 + d_2\eta), \quad 20$$

where $0 \le \eta \le 1$, $d_2 = \frac{L_2}{L_3}$, and $d_3 = \frac{L_3}{L}$. Assuming a thin phase screen implies that $d_2 = \frac{L_2}{L_3} << 1$ and since $0 \le \eta \le 1$, then (20) simplifies to $d_3(1 + d_2\eta) \cong d_3$. (Refer back to the section on random phase screen model.) As a result, the scintillation index (11) becomes

$$\sigma_I^2(\vec{r}, L) = 8\pi^2 k^2 L d_2 d_3 \int_0^\infty \kappa \Phi_n(\kappa) \exp\left(-\frac{\Lambda L \kappa^2 d_3^2}{k}\right)\left\{I_0(2\Lambda r \kappa d_3) - \cos\left[\frac{L\kappa^2}{k} d_3\left(1 - \overline{\Theta} d_3\right)\right]\right\} d\kappa. \quad 21$$

Again separating the scintillation index into two integrals, the radial and longitudinal components are identified as

$$\hat{\sigma}_{I,r}^2(\vec{r}, L) = 8\pi^2 k^2 L d_2 d_3 \int_0^\infty \kappa \Phi_n(\kappa) \exp\left[-\frac{\Lambda L \kappa^2 d_3^2}{k}\right]\{I_0(2\Lambda r \kappa d_3) - 1\} d\kappa, \quad 22$$

and

$$\hat{\sigma}_{I,l}^2(\vec{r}, L) = 8\pi^2 k^2 L d_2 d_3 \int_0^\infty \kappa \Phi_n(\kappa) \exp\left[-\frac{\Lambda L \kappa^2 d_3^2}{k}\right]\left\{1 - \cos\left[\frac{L\kappa^2}{k} d_3\left(1 - \overline{\Theta} d_3\right)\right]\right\} d\kappa. \quad 23$$

Evaluating the integrals, see appendix B, radial and longitudinal components can be simplified to

$$\hat{\sigma}_{I,r}^2(\vec{r}, L) = 6.45 \hat{\sigma}_R^2 (\Lambda d_3)^{5/6} \frac{r^2}{W^2}, \quad 24$$

and

$$\hat{\sigma}_{I,l}^2(\vec{r}, L) = 3.87 \hat{\sigma}_R^2 \left\{\left[(\Lambda d_3)^2 + \left(1 - \overline{\Theta} d_3\right)^2\right]^{5/12} \cos\left[\frac{5}{6} \tan^{-1}\left(\frac{1 - \overline{\Theta} d_3}{\Lambda d_3}\right)\right] - (\Lambda d_3)^{5/6}\right\}, \quad 25$$

where $\hat{\sigma}_R^2 = 2.25\hat{C}_n^2 L^{11/6} d_2 d_3^{11/6}$ is the Rytov variance for the thin phase screen model. By combining the radial and longitudinal components, the total scintillation index under the thin phase screen model is approximately

$$\hat{\sigma}_R^2(\vec{r}, L) \cong 6.45\hat{\sigma}_R^2(\Lambda d_3)^{5/6} \frac{r^2}{W^2} + 3.87\hat{\sigma}_R^2 \left\{ \left[(\Lambda d_3)^2 + (1 - \overline{\Theta} d_3)^2 \right]^{5/12} \times \cos\left[\frac{5}{6} \tan^{-1}\left(\frac{1 - \overline{\Theta} d_3}{\Lambda d_3} \right) \right] - (\Lambda d_3)^{5/6} \right\}. \quad 26$$

It has been shown by Andrews [5] that (26) closely approximates (18) when the phase screen position satisfies

$$d_3 = 0.67 - 0.17\Theta. \quad 27$$

Plane wave models have beam parameters of $\Theta = 1$ and $\Lambda = 0$, which implies that the screen would be placed so that $d_3 = 0.5$. Spherical wave models have beam parameters of $\Theta = 0$ and $\Lambda = 0$, thus screen placement requires that $d_3 = 0.67$. For collimated beams, we see that $0.5 < d_3 < 0.67$. So, for a collimated beam the screen must be closer to the transmitter than for a plane wave. Figure 9 shows a comparison of a collimated beam passing through an extended medium model and a thin random phase screen model. [5]

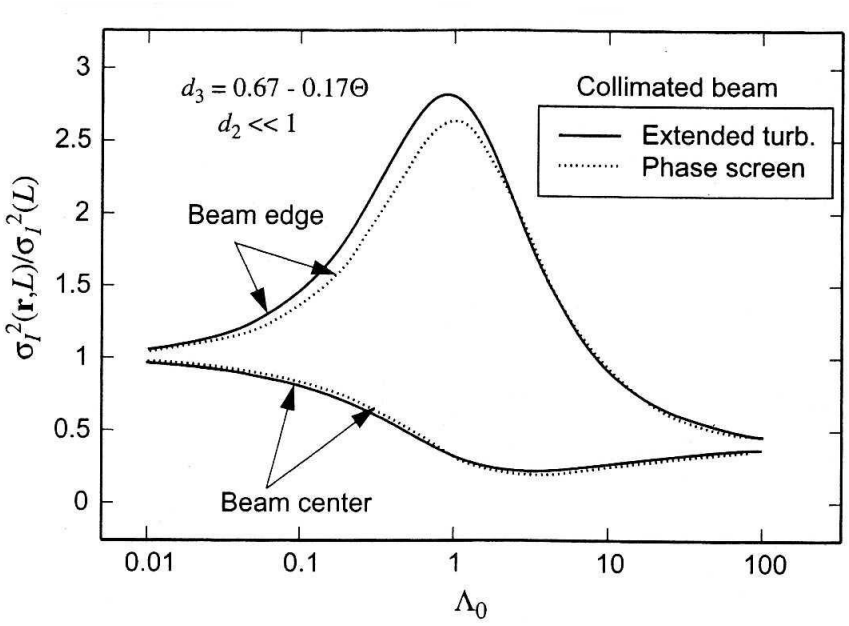

Figure 9 : The curves are the scaled scintillation index for a collimated beam and are plotted as a function $\Lambda_0 = \frac{2L}{kW_0^2}$.

COVARIANCE FUNCTION OF IRRADIANCE FLUCTUATIONS

The covariance function of irradiance fluctuations describes how irradiance fluctuations at one point in the beam are correlated with those at another point. Let $\vec{r}_1$ and $\vec{r}_2$ denote the two points in the receiver plane. Using the extended medium model I has been shown that the covariance function is expressed as [5]

$$B_I(\vec{p},\vec{r},L) = 8\pi^2 k^2 L \int_0^1 \int_0^\infty \kappa \Phi_n(\kappa) \exp\left(-\frac{\Lambda L \xi^2 \kappa^2}{k}\right) \mathrm{Re}\left\{ J_0\left[\kappa\left|\left(1-\overline{\Theta}\xi\right)\vec{p} - 2i\Lambda\xi\vec{r}\right|\right] - \exp\left[-\frac{iL\kappa^2}{k}\xi\left(1-\overline{\Theta}\xi\right)\right] J_0\left[\left(1-\overline{\Theta}\xi - i\Lambda\xi\right)\rho\kappa\right]\right\} d\kappa d\xi, \quad 28$$

where $J_0(z)$ denotes the Bessel function of the first kind, see A16 in appendix A, $\vec{r} = \frac{1}{2}(\vec{r}_1 + \vec{r}_2)$, $\vec{p} = \vec{r}_1 - \vec{r}_2$, $r = |\vec{r}|$, $\rho = |\vec{p}|$, and the normalized distance for $0 \le z \le L$ is given as $\xi = 1 - \frac{z}{L}$, so that $0 \le \xi \le 1$. In addition, the absolute value in the Bessel function refers to the magnitude of the vector expression, not the complex expression. Equation (28) can be described as a spatial statistic because of the spatial points in the beam, $\vec{r}_1$ and $\vec{r}_2$. However, temporal statistics are measured in most applications. The *Taylor frozen turbulence hypothesis* suggests that turbulent eddies are treated as being frozen in space and are being moved across the path of observation by wind speed, denoted as $V_\perp$. Knowledge of the average wind speed transverse to the direction of the propagation will allow us to convert spatial statistics into temporal statistics. Under the frozen turbulence hypothesis, the covariance function is approximated as, see appendix C,

$$B_I(\tau,r,L)=8\pi^2k^2L\int_0^1\int_0^\infty \kappa\Phi_n(\kappa)\exp\left(-\frac{\Lambda L\xi^2\kappa^2}{k}\right)\mathrm{Re}\left\{J_0\left[\kappa V_\perp\tau\right]\left(I_0\left[2\Lambda\kappa\xi\overline{r}\right]\right.\right.$$
$$\left.\left.-\exp\left[-\frac{iL\kappa^2}{k}\xi\left(1-\overline{\Theta}\xi\right)\right]\right)\right\}d\kappa d\xi\,. \qquad 29$$

By separating (29) into two integrals, we can identify the radial and longitudinal components as, (C1) and (C2) respectively,

$$B_{I,r}(\tau,r,L)=8\pi^2k^2L\int_0^1\int_0^\infty \kappa\Phi_n(\kappa)\exp\left(-\frac{\Lambda L\xi^2\kappa^2}{k}\right)J_0\left[\kappa V_\perp\tau\right]\left(I_0\left[2\Lambda\kappa\xi\overline{r}\right]-1\right)d\kappa d\xi\,, \qquad 30$$

and

$$B_{I,l}(\tau,r,L)=8\pi^2k^2L\int_0^1\int_0^\infty \kappa\Phi_n(\kappa)\exp\left(-\frac{\Lambda L\xi^2\kappa^2}{k}\right)\mathrm{Re}\left\{J_0\left[\kappa V_\perp\tau\right]\right.$$
$$\left.\times\left(1-\exp\left[-\frac{iL\kappa^2}{k}\xi\left(1-\overline{\Theta}\xi\right)\right]\right)\right\}d\kappa d\xi\,. \qquad 31$$

Observe that (31) does not depend on $\vec{r}$, so setting $\vec{r}=0$ leaves the longitudinal component of irradiance fluctuations as a temporal statistic

$$B_{I,l}(\tau,L)=8\pi^2k^2L\int_0^1\int_0^\infty \kappa\Phi_n(\kappa)\exp\left(-\frac{\Lambda L\xi^2\kappa^2}{k}\right)\mathrm{Re}\left\{J_0\left[\kappa V_\perp\tau\right]\right.$$
$$\left.\times\left(1-\exp\left[-\frac{iL\kappa^2}{k}\xi\left(1-\overline{\Theta}\xi\right)\right]\right)\right\}d\kappa d\xi\,. \qquad 32$$

For the extended medium model, an exact result for the covariance function using the Kolmogorov power-law spectrum has not yet been derived. However, applying the thin phase

screen model to (29) simplifies the covariance function from evaluating two integrals to evaluating one integral

$$B_I(\tau,r,L)=8\pi^2k^2Ld_2d_3\int_0^\infty \kappa\Phi_n(\kappa)\exp\left(-\frac{\Lambda Ld_3^2\kappa^2}{k}\right)\mathrm{Re}\left\{J_0\left[\kappa V_\perp\tau\right]\right.$$
$$\left.\times\left(I_0\left[2\Lambda\kappa d_3r\right]-\exp\left[-\frac{iL\kappa^2}{k}d_3\left(1-\overline{\Theta}d_3\right)\right]\right)\right\}d\kappa. \qquad 33$$

The radial and longitudinal components of the covariance function under the thin phase screen model are

$$B_{I,r}(\tau,r,L)=8(0.033)\pi^2\hat{C}_n^2k^2Ld_2d_3\int_0^\infty \kappa^{-8/3}\exp\left(-\frac{\Lambda Ld_3^2\kappa^2}{k}\right)J_0\left(\kappa V_\perp\tau\right)\left(I_0\left[2\Lambda\kappa d_3r\right]-1\right)d\kappa, \qquad 34$$

and

$$B_{I,l}(\tau,L)=8\pi^2k^2Ld_2d_3\int_0^\infty \kappa\Phi_n(\kappa)\exp\left(-\frac{\Lambda Ld_3^2\kappa^2}{k}\right)\mathrm{Re}\left\{J_0\left[\kappa V_\perp\tau\right]\right.$$
$$\left.\times\left(1-\exp\left[-\frac{iL\kappa^2}{k}d_3\left(1-\overline{\Theta}d_3\right)\right]\right)\right\}d\kappa. \qquad 35$$

Again, the radial component contains both spatial and temporal arguments, while the longitudinal component contains a temporal argument. Upon evaluating the integrals, see appendix D, the radial and longitudinal components are simplified and approximated to

$$B_{I,r}(\tau,r,L)\cong 6.45\,\hat{\sigma}_R^2\left(\Lambda d_3\right)^{5/6}\left(\frac{r}{W}\right)^2{}_1F_1\left(\frac{1}{6};1;-\frac{\omega_t^2\tau^2}{4\Lambda d_3^2}\right), \qquad 36$$

and

$$B_{I,l}(\tau,L)=3.8637\hat{\sigma}_R^2\,\mathrm{Re}\left\{i^{5/6}\left[1-\left(\overline{\Theta}+i\Lambda\right)d_3\right]^{5/6}{}_1F_1\left(-\frac{5}{6};1;-\frac{\omega_t^2\tau^2}{4id_3\left[1-\left(\overline{\Theta}+i\Lambda\right)d_3\right]}\right)\right.$$
$$\left.-\left(\Lambda d_3\right)^{5/6}{}_1F_1\left(-\frac{5}{6};1;-\frac{\omega_t^2\tau^2}{4\Lambda d_3^2}\right)\right\}, \qquad 37$$

where ${}_pF_q(z)$ denotes a generalized hypergeometric function, see A16 in appendix A. In addition, $d_3=0.67-0.17\Theta$, $\omega_t=\dfrac{V_\perp}{\sqrt{L/k}}$ is the Fresnel frequency, and $\hat{\sigma}_R^2=2.25\hat{C}_n^2L^{11/6}d_2d_3^{11/6}$ is the Rytov variance for the thin phase screen model. It is common to define additional parameters to simplify the arguments of the ${}_1F_1$ hypergeometric functions; let $a_1=\dfrac{1}{4d_3i\left[1-\left(\overline{\Theta}+i\Lambda\right)d_3\right]}$ and $a_2=\dfrac{1}{4\Lambda d_3^2}$. Using these additional parameters, then (36) and (37) are simplified to

$$B_{I,r}(\tau,r,L)\cong 6.45\hat{\sigma}_R^2\left(\Lambda d_3\right)^{5/6}\left(\frac{r}{W}\right)^2{}_1F_1\left(\frac{1}{6};1;-a_2\omega_t^2\tau^2\right), \qquad 38$$

and

$$B_{I,l}(\tau,L)=3.8637\hat{\sigma}_R^2\,\mathrm{Re}\left\{i^{5/6}\left[1-\left(\overline{\Theta}+i\Lambda\right)d_3\right]^{5/6}{}_1F_1\left(-\frac{5}{6};1;-a_1\omega_\perp^2\tau^2\right)\right.$$
$$\left.-\left(\Lambda d_3\right)^{5/6}{}_1F_1\left(-\frac{5}{6};1;-a_2\omega_t^2\tau^2\right)\right\}. \qquad 39$$

By combining (38) and (39), we have the total covariance function of irradiance fluctuations,

$$B_I(\tau, r, L) \cong 6.45\,\hat{\sigma}_R^2 (\Lambda d_3)^{5/6} \left(\frac{r^2}{W^2} \right) {}_1F_1\left(\frac{1}{6}; 1; -a_2 \omega_t^2 \tau^2 \right)$$

$$+ 3.8637\ \hat{\sigma}_R^2\ \mathrm{Re}\left\{ i^{5/6} \left[1 - (\overline{\Theta} + i\Lambda) d_3 \right]^{5/6} {}_1F_1\left(-\frac{5}{6}; 1; -a_1 \omega_t^2 \tau^2 \right) - (\Lambda d_3)^{5/6} {}_1F_1\left(-\frac{5}{6}; 1; -a_2 \omega_t^2 \tau^2 \right) \right\}. \quad 40$$

TEMPORAL SPECTRUM OF IRRADIANCE

The temporal spectrum of irradiance fluctuations is an important characteristic of atmospheric noise associated with optical communication systems and laser radar systems. It is defined by the Fourier transform of the temporal covariance function

$$S_I(\omega) = 2\int_{-\infty}^{\infty} B_I(\tau, L) e^{-i\omega\tau} d\tau = 4\int_{0}^{\infty} B_I(\tau, L)\cos(\omega\tau) d\tau, \qquad 41$$

where $B_I(\tau, L)$ is the temporal covariance function of irradiance fluctuations. The extra factor of 2 in the transform integral is due to considering only positive frequencies and the using the real component of the complex exponential is due to the even property of the covariance function with respect to τ. In addition, the temporal spectrum is a function of ω, which represents angular frequency.

We have the radial and longitudinal components of the covariance functions for the irradiance fluctuations, (38) and (39). Substituting (38) and (39) into (41) yields

$$S_{I,r}(\omega) = 4(6.45)\hat{\sigma}_R^2 (\Lambda d_3)^{5/6} \left(\frac{r^2}{W^2}\right) \int_0^{\infty} {}_1F_1\left(\frac{1}{6}; 1; -\frac{\omega_t^2 \tau^2}{4\Lambda d_3^2}\right) \cos(\omega\tau) d\tau, \qquad 42$$

and

$$S_{I,l}(\omega) = 4^{1/6}(3.87)\hat{\sigma}_R^2 d_3^{-5/6} \operatorname{Re}\left\{ a_1^{-5/6} \int_0^{\infty} {}_1F_1\left(-\frac{5}{6}; 1; -a_1\omega_t^2\tau^2\right) \cos(\omega\tau) d\tau \right\}$$
$$- 4(3.87)\hat{\sigma}_R^2 (\Lambda d_3)^{5/6} \operatorname{Re}\left\{ \int_0^{\infty} {}_1F_1\left(-\frac{5}{6}; 1; -a_2\omega_t^2\tau^2\right) \cos(\omega\tau) d\tau \right\}, \qquad 43$$

where ${}_pF_q(z)$ denotes a generalized hypergeometric function, see A16 in appendix A,

$a_1 = \dfrac{1}{4d_3 i\left[1-\left(\overline{\Theta}+i\Lambda\right)d_3\right]}$, $a_2 = \dfrac{1}{4\Lambda d_3^2}$, $\omega_t = \dfrac{V_\perp}{\sqrt{L/k}}$ is the Fresnel frequency, and

$d_3 = 0.67 - 0.17\Theta$. Evaluating (42) and (43), see appendix E, the radial and longitudinal components of the temporal spectrum of irradiance are approximated by

$$S_{I,r}(\omega) = 19.4924\hat{\sigma}_R^2 \frac{\Lambda d_3^{7/6}}{\omega_t}\left(\frac{r^2}{W^2}\right)\left(\frac{\omega}{\omega_t}\right)^{-2/3}\left\{{}_1F_1\left(\frac{1}{6};\frac{2}{3};-\frac{\Lambda d_3^2\omega^2}{\omega_t^2}\right)\right.$$
$$\left. - 0.965722\left(\Lambda d_3^2\right)^{1/3}\left(\frac{\omega}{\omega_t}\right)^{2/3}{}_1F_1\left(\frac{1}{2};\frac{4}{3};-\frac{\Lambda d_3^2\omega^2}{\omega_t^2}\right)\right\}, \qquad 44$$

and

$$S_{I,l}(\omega) = \frac{3.90\hat{\sigma}_R^2}{\omega_t d_3^{5/6}}\,\mathrm{Re}\left\{\left[\frac{\omega}{\omega_t}\right]^{-8/3}\left[{}_1F_1\left(-\frac{5}{6};-\frac{1}{3};-\frac{\omega^2}{4a_2\omega_t^2}\right) - {}_1F_1\left(-\frac{5}{6};-\frac{1}{3};-\frac{\omega^2}{4a_1\omega_t^2}\right)\right]\right.$$
$$\left. + 0.29\left[\frac{1}{a_2^{4/3}}{}_1F_1\left(\frac{1}{2};\frac{7}{3};-\frac{\omega^2}{4a_2\omega_t^2}\right) - \frac{1}{a_1^{4/3}}{}_1F_1\left(\frac{1}{2};\frac{7}{3};-\frac{\omega^2}{4a_1\omega_t^2}\right)\right]\right\}. \qquad 45$$

Thus the total temporal spectrum model is the sum of (44) and (45),

$$S_I(\omega) = S_{I,r}(\omega, r) + S_{I,l}(\omega). \qquad 46$$

Now that we have an expression for the temporal spectrum of irradiance fluctuations, we want to investigate the maximum width of spectrum. Observe in equations (44) and (45), the expression $\frac{\omega}{\omega_t}$. The Fresnel frequency defined by $\omega_t = \dfrac{V_\perp}{\sqrt{L/k}}$ plays an important role in determining the

width of the spectrum. In weak turbulence, we often identify spectral width with ω_t and from the definition of the Fresnel frequency we see that the spectral width varies with the wave number. Andrews [5] has shown the temporal spectrum can be plotted as a function of the expression $\frac{\omega}{\omega_t}$, see Figure 10.

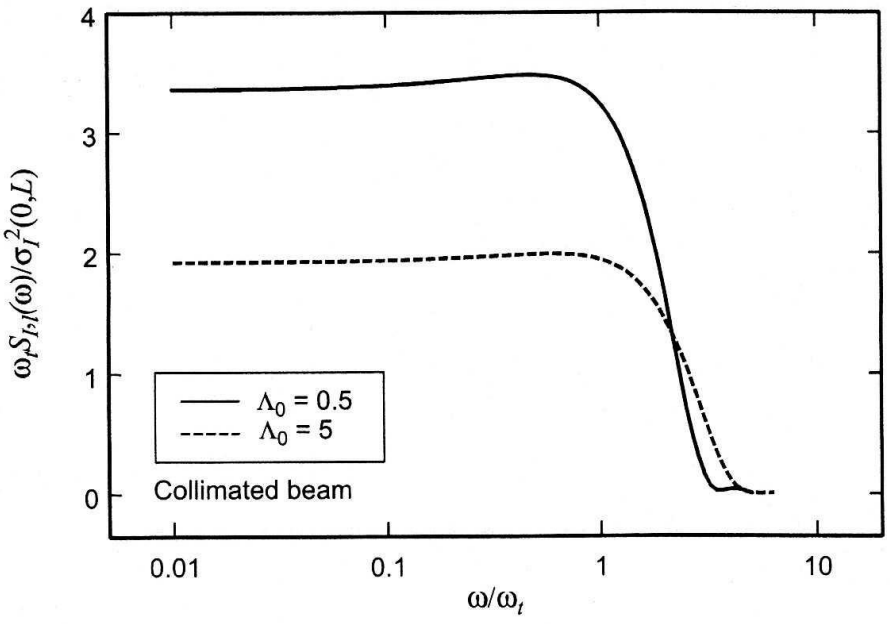

Figure 10: Power spectrum of irradiance fluctuations of a collimated beam scaled by the on-axis scintillation index and multiplied by ω_t. Results are for *r* = 0 and the Kolmogorov power-law spectrum.

Figure 10 shows the spectrum to drop off when $\frac{\omega}{\omega_t} \cong 1$. It is common to describe the width of the spectrum when the frequency, ω, is approximately equal to the Fresnel frequency, ω_t. However, using the Fresnel frequency to describe the width of the spectrum does not capture the contribution of the spectrum when $\omega > \omega_t$. One way to increase the amount of contribution when investigating the spectrum's width is the intersection of the constant function $\frac{1}{e^2}$ with the spectrum. Thus, we will consider the spectrum's width in two ways, using the Fresnel frequency

and the constant function $\frac{1}{e^2}$. In the next section, we will define the quasi-frequency and investigate how the quasi-frequency is related to the width of the spectrum.

QUASI-FREQUENCY

Laser communication systems are one of many applications of transmitting optical waves through the atmosphere. A laser communication system is composed of three subsystems; a transmitter, a channel, and a receiver. The purpose of the transmitter is to prepare information to be sent on an optical wave, while the channel is simply the transmission medium between the transmitter and receiver. The receiver is designed to collect the optical wave, process the wave, and convert it into an electrical current in order to recover the transmitted information. There are two basic types of receivers, the first is a direct (or power) detecting receiver, which detects only the intensity of the wave, and the second is a coherent receiver, which detects the wave itself. One of the most important concerns with laser communication systems is signal detection. Fluctuations in the beam's intensity could result in the receiver processing or missing the transmitted signal. However, a receiver may collect light from another source besides the transmitter. Signals produced from the unwanted light are referred to as noise, and produce false alarms in the receiver. A threshold is a value that can be set in order to maximize the probability of detection while minimizing the probability of missed detection. However, maximizing the probability of detection results in an increase of the amount of false alarms. Thus, the concept of a signal-to-noise ratio (SNR) is very important when studying laser communication systems. By graphing the output current of the detector, we see that current randomly fluctuates with respect to time, see Figure 11. A fade occurs when the desired current drops below the threshold level, while a surge occurs when the current rises above the threshold level. The frequency of fades and surges are of particular interest when studying the detection process. Rice [6; 7; 8] has shown

that for a stationary process the frequency in which the output current makes a positive or negative crossing across the

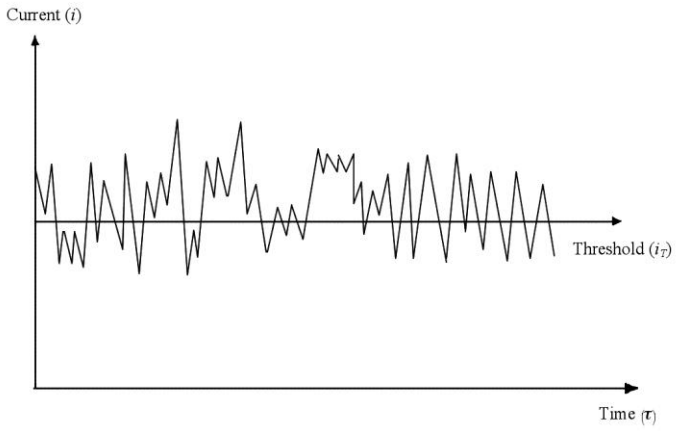

Figure 11: Example of output current from detector over time.

threshold value (i_T) is given by the mean expected number of crossings per second defined by

$$\langle n(i_T)\rangle = \frac{1}{2}\int_{-\infty}^{\infty}|i'|p_{s+n}(i_T,i')di', \qquad 47$$

where $p_{s+n}(i,i')$ is the joint probability density function of the output current i and its time derivative i'. In addition, Rice showed that the time derivative of a random process and the process itself are uncorrelated, while not necessarily being independent. If we assume that $i(\tau)$ is a Gaussian random process, then by the definition of a derivative we know that $i'(\tau)$ is a Gaussian process as well. It has been shown that fading statistics can be based on statistics

associated with the irradiance of the received wave and (47) can be expressed in terms of irradiance, *I*, as

$$\langle n(I_T)\rangle = \frac{1}{2}\int_{-\infty}^{\infty}|I'|p_I(I_T, I')dI' \qquad 48$$

where $p_I(I,I')$ is the joint probability density function of irradiance *I* and its derivative I', and I_T represents a prescribed threshold value. Evaluating (48) leads to the mean expected number of fades per unit time to be expressed as

$$\langle n(I_T)\rangle = \frac{1}{2\pi}\sqrt{\frac{b_2}{b_0}}\exp\left[-\frac{\left(\left(1/2\right)b_0 - 0.23F_T\right)^2}{2b_0}\right] = \nu_0 \exp\left[-\frac{\left(\left(1/2\right)b_0 - 0.23F_T\right)^2}{2b_0}\right], \qquad 49$$

where F_T is the fade threshold parameter, ν_0 is called the quasi-frequency, $b_2 = -B_I''(0)$, and $b_0 = B_I(0)$.[5] The fade parameter F_T, measured in decibels (dB), represents the decibel level below the on-axis mean irradiance that the threshold I_T is set. From (49), we see that the quasi-frequency is given as

$$\nu_0 = \frac{1}{2\pi}\sqrt{\frac{b_2}{b_0}} = \frac{1}{2\pi}\sqrt{-\frac{B_I''(0)}{B_I(0)}}, \qquad 50$$

and it is measured in hertz. Considering the on-axis characteristics of the beam, it follows that $b_0 = B_{I,I}(0,L)$, which the longitudinal component of the covariance function of irradiance (37) when $\tau = 0$. By twice differentiating (37) with respect to time and setting $\tau = 0$, we have

$b_2 = -B''_{I,l}(0,L)$. Applying the inverse Fourier transform to the longitudinal component of the covariance function (45) gives

$$B_{I,l}(\tau, L) = \int_{-\infty}^{\infty} e^{i\omega\tau} S_{I,l}(\omega) d\omega,$$

and when $\tau = 0$ it follows that

$$b_0 = B_{I,l}(0, L) = \frac{1}{2\pi} \int_0^{\infty} S_{I,l}(\omega) d\omega. \quad 51$$

Similarly, for second derivative we have

$$B''_{I,l}(\tau, L) = -\int_{-\infty}^{\infty} \omega^2 e^{i\omega\tau} S_{I,l}(\omega) d\omega,$$

and when $\tau = 0$ then

$$b_2 = -B''_{I,l}(0, L) = \frac{1}{2\pi} \int_0^{\infty} \omega^2 S_{I,l}(\omega) d\omega. \quad 52$$

For on-axis beam characteristics, we can use (51) and (53) to calculate the quasi-frequency v_0 using the covariance function when $\tau = 0$

$$v_0 = \frac{1}{2\pi} \sqrt{-\frac{B''_{I,l}(0, L)}{B_{I,l}(0, L)}} \quad 53$$

or using the temporal spectrum of irradiance

$$\nu_0 = \frac{1}{2\pi}\left[\frac{\int_0^\infty \omega^2 S_{I,l}(\omega)d\omega}{\int_0^\infty S_{I,l}(\omega)d\omega}\right]^{1/2}. \qquad 54$$

Assuming that $\int_0^\infty S_{I,l}(\omega)d\omega$ is a finite value, it is the area under the curve for the longitudinal component of the spectrum. Consequently, the expression

$$\frac{S_{I,l}(\omega)}{\int_0^\infty S_{I,l}(\omega)d\omega} \qquad 55$$

represents the normalized longitudinal component of temporal spectrum of irradiance fluctuations, which we denote as $\hat{S}_{I,l}(\omega)$. Using the notation for the normalized spectrum, (54) can be written as

$$\nu_0 = \frac{1}{2\pi}\left[\int_0^\infty \omega^2 \hat{S}_{I,l}(\omega)d\omega\right]^{1/2}. \qquad 56$$

Investigating the normalized spectrum defined by (55) reveals that it has properties similar to a probability density function. By treating (55) as a probability density function we can use statistical analysis to describe characteristics about the normalized spectrum. While a mean value is a first-order statistical moment that a value around which most other values tend to cluster, second-order moments are used to describe the distribution pattern around the mean value. The variance is an important second-order moment and for the normalized spectrum the variance is defined as

$$\sigma^2 = \int_0^\infty \omega^2 \hat{S}_{I,l}(\omega) d\omega . \qquad 57$$

Taking the square root of both sides of (57) we have the standard deviation, given as

$$\sigma = \left[\int_0^\infty \omega^2 \hat{S}_{I,l}(\omega) d\omega \right]^{1/2}, \qquad 58$$

this roughly measures the width of a probability density function (PDF). By comparing (56) and (58), we see that $2\pi\nu_0$ is the width of the normalized longitudinal component of the temporal spectrum of irradiance, if it were treated as a PDF.

Treating (55) as a PDF, let's compare the maximum width of the normalized longitudinal component of the temporal spectrum, calculated used the constant e^{-2}, to the quasi-frequency for collimated beams. Figure 12 shows the normalized spectrums for two collimated beams with spot sizes of 1.5 cm and 3 cm. The intersection of the spectrums with the constant function e^{-2} is one way to describe the width of the spectrum.

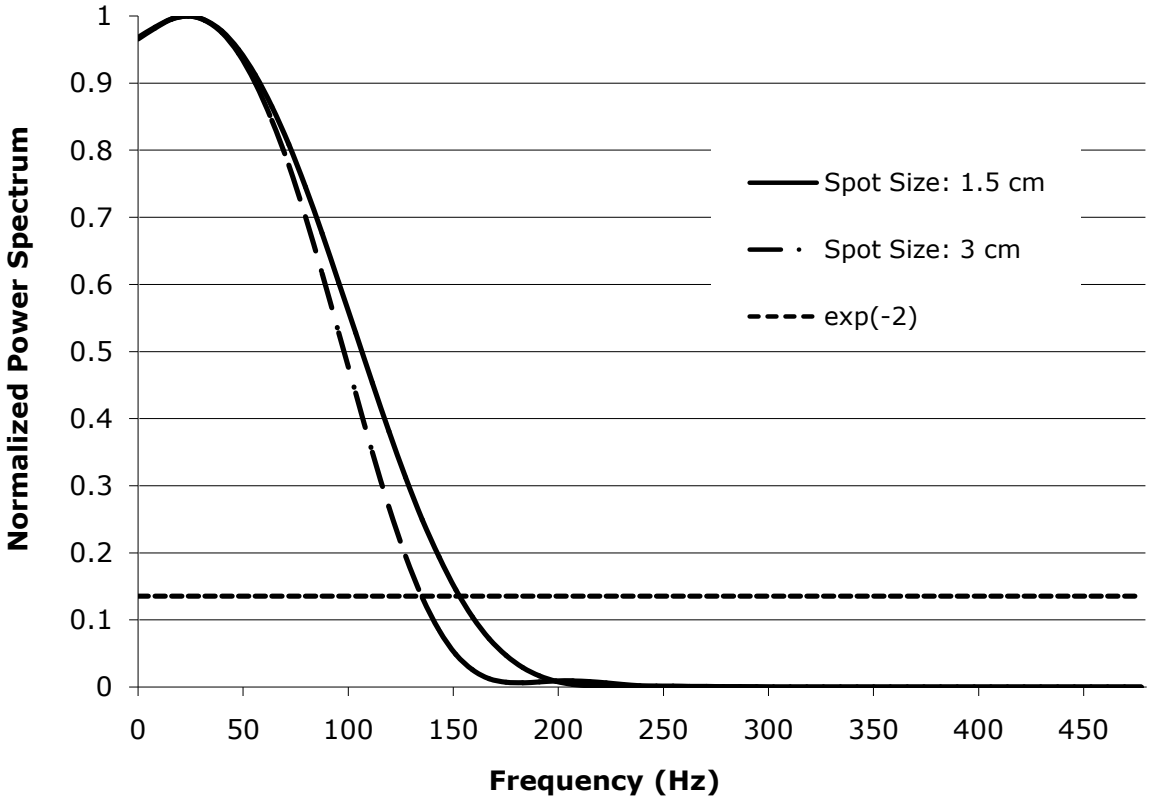

Figure 12: Normalized longitudinal component of the power spectrum of irradiance fluctuations for collimated beams with spot sizes 1.5 cm and 3 cm, propagating 1000 m, and constant function e^{-2}.

The graphs of the normalized spectrums indicate possible convergence of the spectrum, however as $S_{I,l}(\omega)$ approaches infinity there are small fluctuations above the ω axis. Consequently, integrating (45),

$$S_{I,l}(\omega) = \frac{3.90\hat{\sigma}_R^2}{\omega_t d_3^{5/6}} \operatorname{Re}\left\{\left[\frac{\omega}{\omega_t}\right]^{-8/3}\left[{}_1F_1\left(-\frac{5}{6};-\frac{1}{3};-\frac{\omega^2}{4a_2\omega_t^2}\right) - {}_1F_1\left(-\frac{5}{6};-\frac{1}{3};-\frac{\omega^2}{4a_1\omega_t^2}\right)\right]\right.$$
$$\left. + 0.29\left[\frac{1}{a_2^{4/3}}{}_1F_1\left(\frac{1}{2};\frac{7}{3};-\frac{\omega^2}{4a_2\omega_t^2}\right) - \frac{1}{a_1^{4/3}}{}_1F_1\left(\frac{1}{2};\frac{7}{3};-\frac{\omega^2}{4a_1\omega_t^2}\right)\right]\right\},$$

over the interval zero to infinity leads to a divergent expression. Considering the physical characteristics of the spectrum suggests that contributing frequencies are over a finite interval. By using manual techniques, we can approximate the width of the spectrum by integrating (45) with respect to angular frequency ω over a finite interval, let's consider the interval [0.01, 3,000]. Earlier, we discussed spectral width using both the Fresnel frequency and the constant e^{-2}. First, let's compare the width of the spectrum using the Fresnel frequency to the quasi-frequency. Our investigation will use collimated beams to wavelengths, 1.55×10^{-6} and 0.532×10^{-6} Additionally, the transverse velocity will be treated as a constant, which is given as $V_{\perp} = 5\,{}^{m}\!/_{s}$. Figures 13 and 14, show the ratio of the width of the normalized longitudinal component of the temporal spectrum of irradiance using the Fresnel frequency,ω_t, compared to the quasi-frequency. The ratio is given as a function of propagation length, L, for collimated beams of various spot sizes with wavelengths of 1.55×10^{-6}.

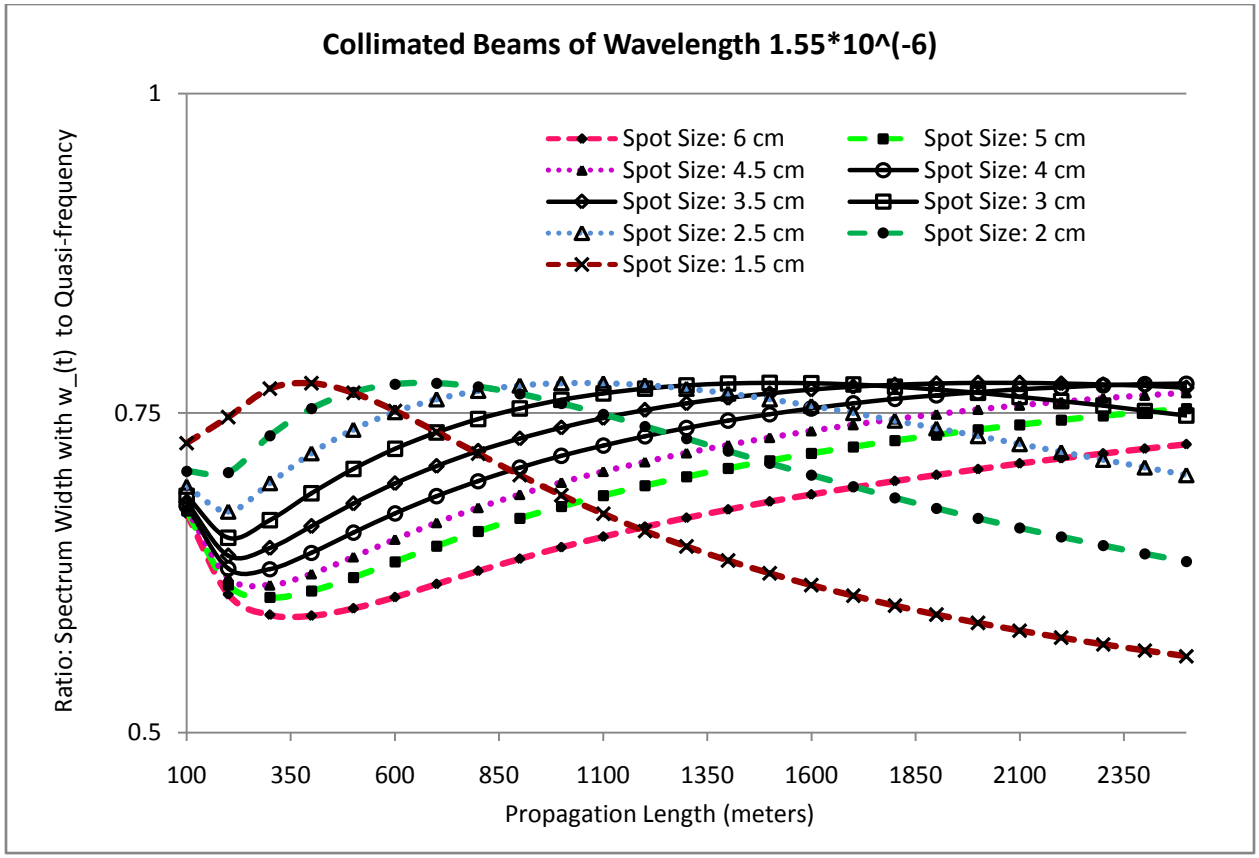

Figure 13: Ratio defined by the width of the $\hat{S}_{I,I}(\omega)$ using the Fresnel frequency scaled by the quasi-frequency. The ratio is a function of propagation length, *L*, for collimated beams with spot sizes 2 cm to 6 cm of wavelengths of 1.55×10^{-6} and transverse velocity is $V_{\perp}=5\,{}^{m}\!/_{s}$.

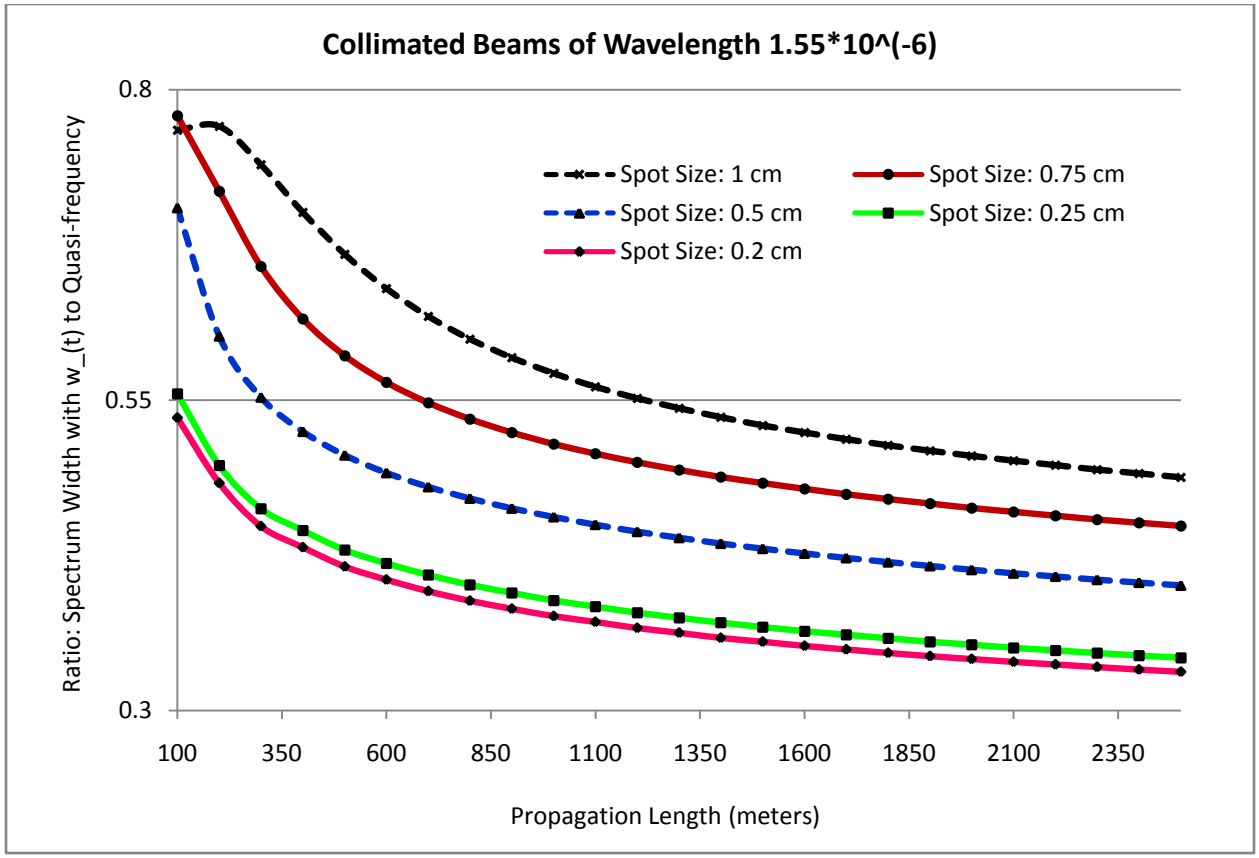

Figure 14: Ratio defined by the width of the $\hat{S}_{I,l}(\omega)$ using the Fresnel frequency scaled by the quasi-frequency. The ratio is a function of propagation length, *L*, for collimated beams with spot sizes 0.2 cm to 1 cm of wavelengths of 1.55×10^{-6} and transverse velocity is $V_{\perp}=5\,{}^{m}\!/_{s}$.

Figures 15 and 16, show the ratio of the width of the normalized longitudinal component of the temporal spectrum of irradiance using the Fresnel frequency,ω_t, compared to the quasi-frequency. Again, the ratio is given as a function of propagation length, *L*, for collimated beams of various spot sizes with wavelengths of 0.532×10^{-6}.

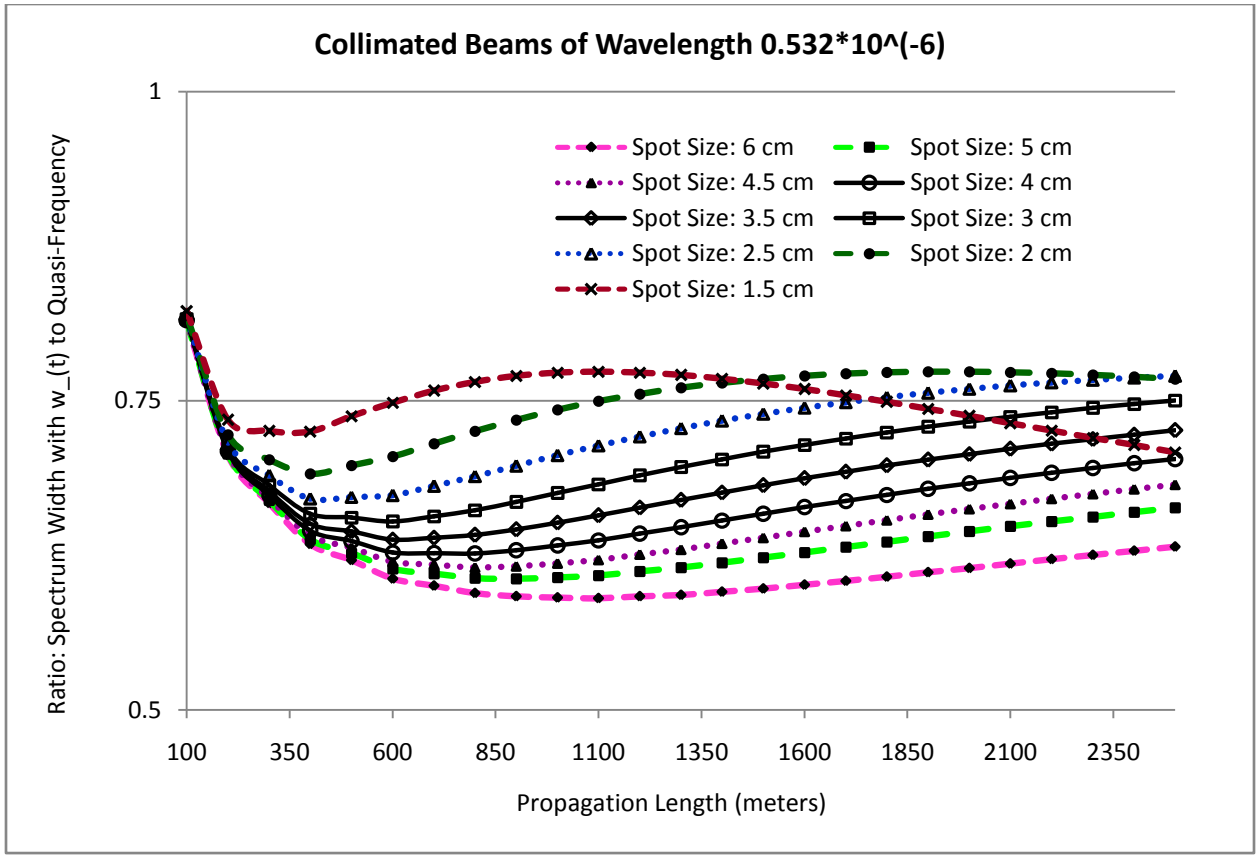

Figure 15: Ratio defined by the width of the $\hat{S}_{I,I}(\omega)$ using the Fresnel frequency scaled by the quasi-frequency. The ratio is a function of propagation length, *L*, for collimated beams with spot sizes 2 cm to 6 cm of wavelengths of 0.532×10^{-6} and transverse velocity is $V_{\perp}=5\,{}^{m}\!/_{s}$.

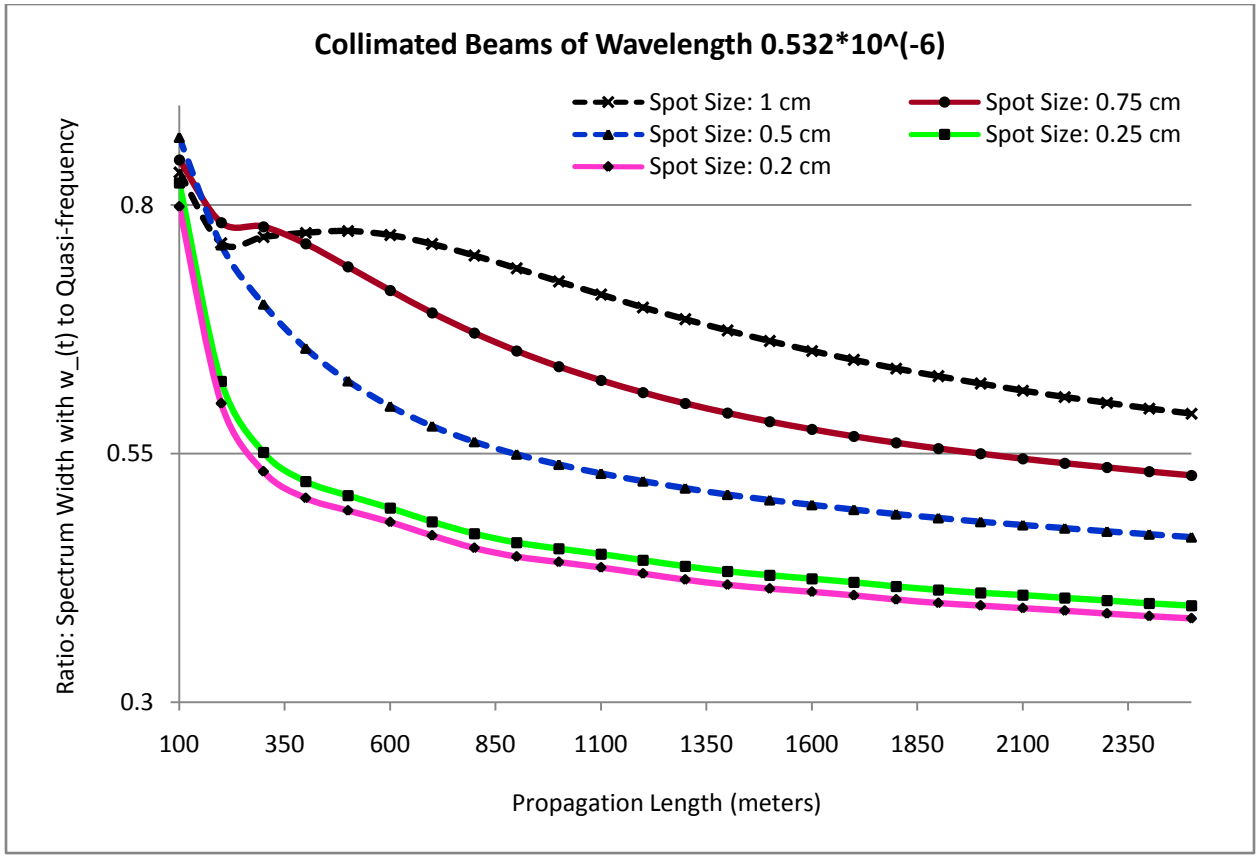

Figure 16: Ratio defined by the width of the $\hat{S}_{I,l}(\omega)$ using the Fresnel frequency scaled by the quasi-frequency. The ratio is a function of propagation length, *L*, for collimated beams with spot sizes 0.2 cm to 1 cm of wavelengths of 0.532×10^{-6} and transverse velocity is $V_{\perp}=5\,m/s$.

Based on the data provided in Figures 13, 14, 15, and 16, comparing the spectrum width using the Fresnel frequency to the quasi-frequency, the spectral width is roughly $\frac{1}{2}v_0$ to $\frac{3}{4}v_0$. Observe that for larger beams and propagation lengths of 1 km, we have a reasonable approximation for the spectral width measured by the Fresnel frequency which is given as $\omega_t \cong \frac{3}{4}v_0$. Recall that quasi-frequency is related to fade statistic calculations. Therefore, we are able to approximate the quasi-frequency by

$$\nu_0 \cong \frac{4}{3}\omega_t = \frac{4V_\perp}{3\sqrt{L/k}}. \qquad 59$$

When calculating the fade statistic given by (49), rather than evaluate (53) or (54) to find the quasi-frequency, one can use (59) to quickly find a reasonable approximation for the quasi-frequency under weak optical turbulence theory.

Now let's compare the width of the spectrum using the constant e^{-2} to the quasi-frequency. Again, we will use collimated beams to wavelengths, 1.55×10^{-6} and 0.532×10^{-6}. Figures 17 and 18 show the ratio of the width of the normalized longitudinal component of the temporal spectrum of irradiance using the constant e^{-2} compared to the quasi-frequency. The ratio is given as a function of propagation length, L, for collimated beams of various spot sizes with wavelengths of 1.55×10^{-6}.

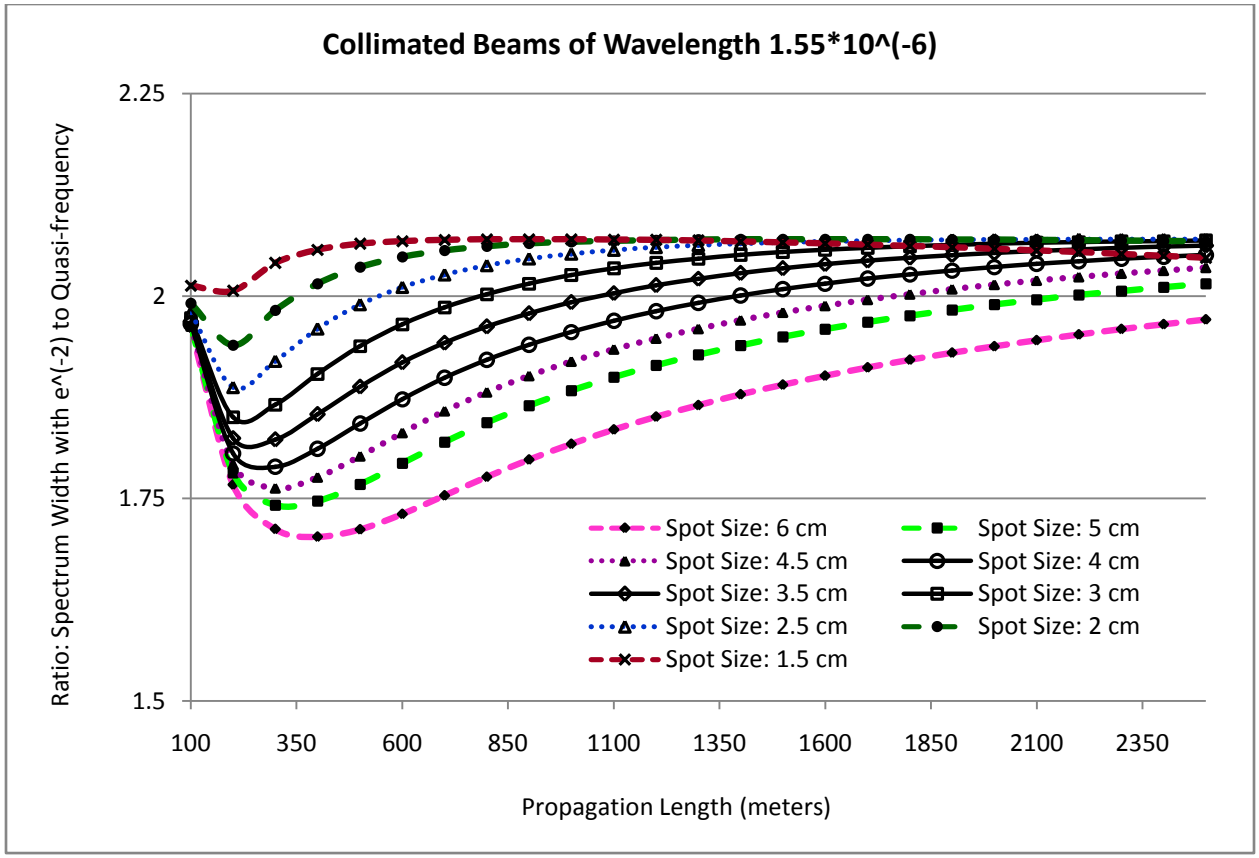

Figure 17: Ratio defined by the width of the $\hat{S}_{I,I}(\omega)$ using the constant e^{-2} scaled by the quasi-frequency. The ratio is a function of propagation length, *L*, for collimated beams with spot sizes 2 cm to 6 cm of wavelengths of 1.55×10^{-6} and transverse velocity is $V_{\perp}=5\,{}^{m}\!/_{s}$.

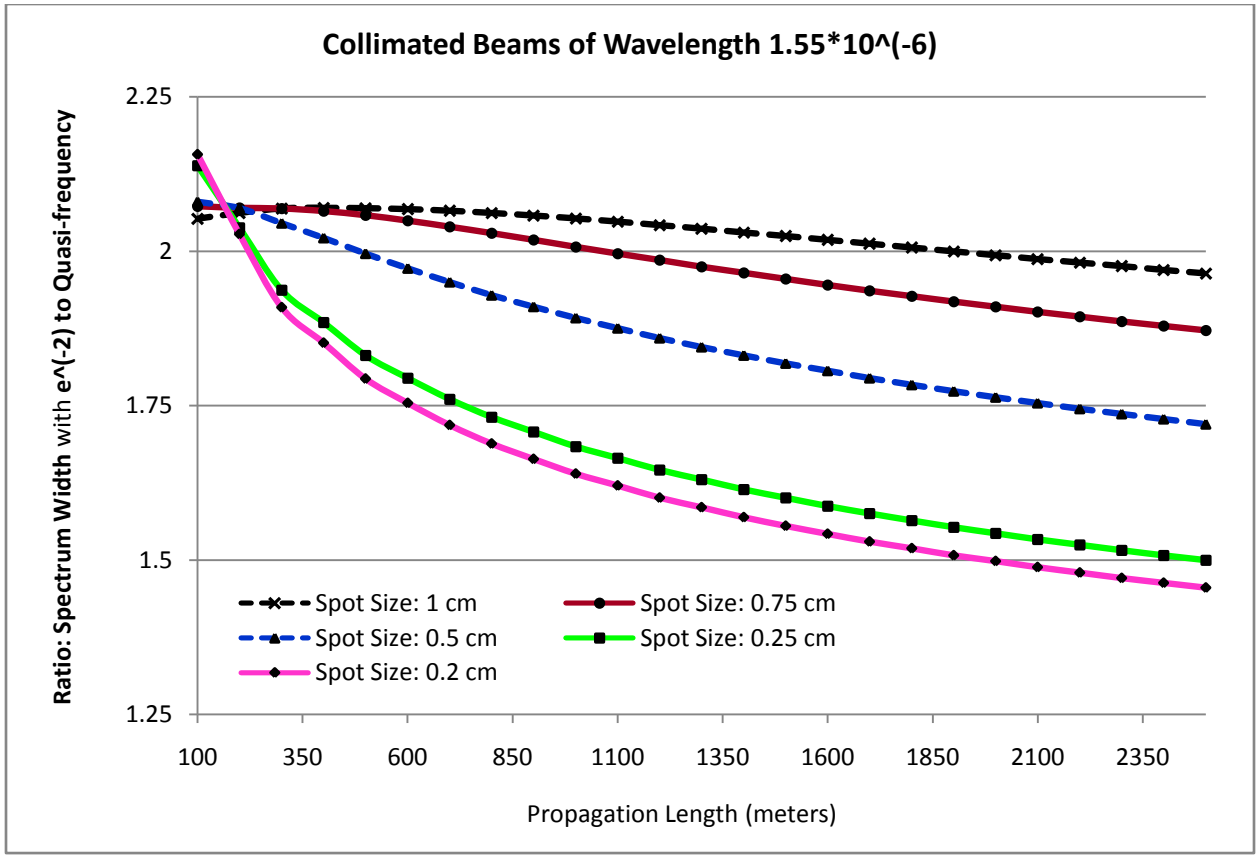

Figure 18: Ratio defined by the width of the $\hat{S}_{I,l}(\omega)$ using the constant e^{-2} scaled by the quasi-frequency. The ratio is a function of propagation length, *L*, for collimated beams with spot sizes 0.2 cm to 1 cm of wavelengths of 1.55×10^{-6} and transverse velocity is $V_{\perp}=5\,{}^{m}\!/_{s}$.

Figures 19 and 20 show the ratio of the width of the normalized longitudinal component of the temporal spectrum of irradiance using the constant e^{-2} compared to the quasi-frequency. Again, the ratio is given as a function of propagation length, *L*, for collimated beams of various spot sizes with wavelengths of 0.532×10^{-6}. Additionally for Figures 19 and 20, observe the propagation axis begins with 200 m rather than 100 m as in the previous figures. Using the phase screen model adds some additional restraints to the model, as a result the propagation length of 100 m violates some assumptions of the phase screen model. Since we are typically

interested in large propagation lengths, generally greater than 100 m, we will not investigate the cause of the erratic values produced at 100 m.

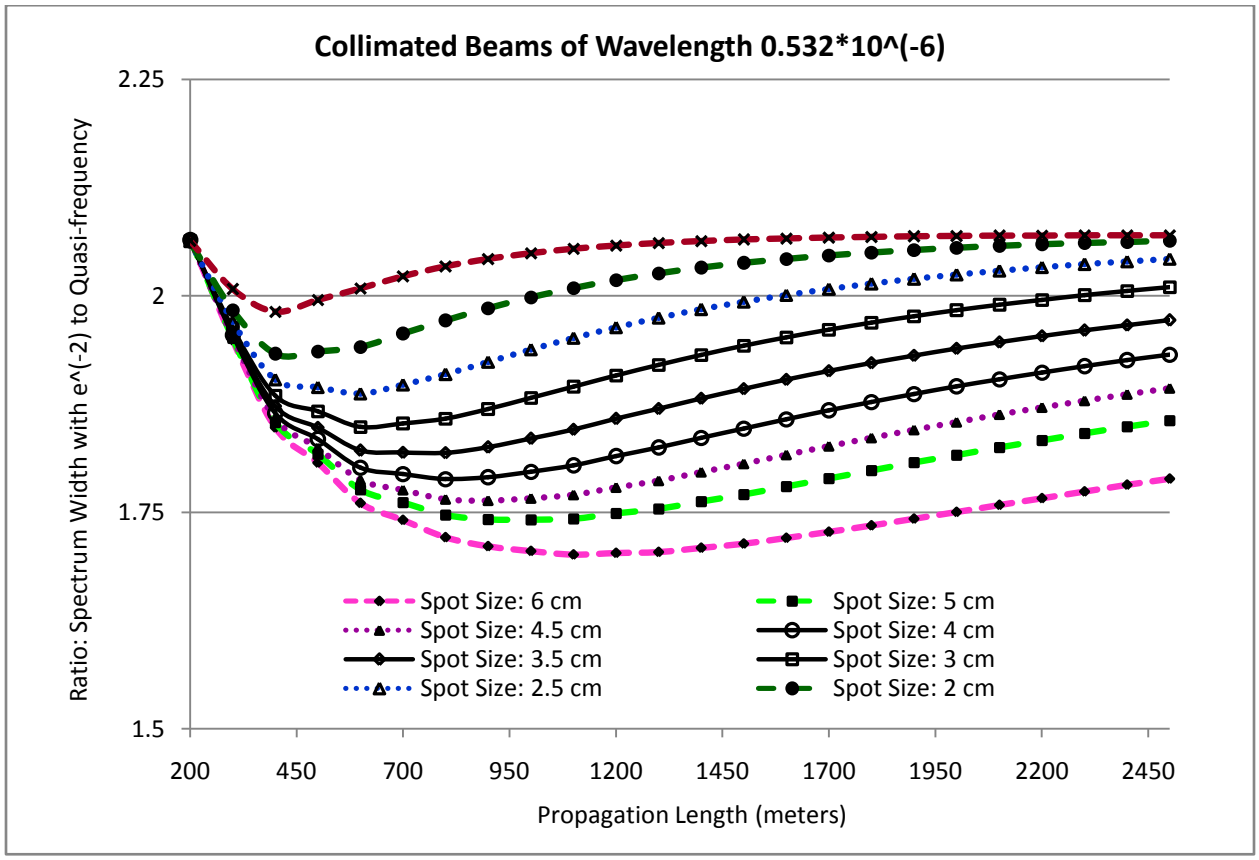

Figure 19: Ratio defined by the width of the $\hat{S}_{I,I}(\omega)$ using constant e^{-2} scaled by the quasi-frequency. The ratio is a function of propagation length, *L*, for collimated beams with spot sizes 2 cm to 6 cm of wavelengths of 0.532×10^{-6} and transverse velocity is $V_{\perp}=5\,{}^{m}\!/_{s}$.

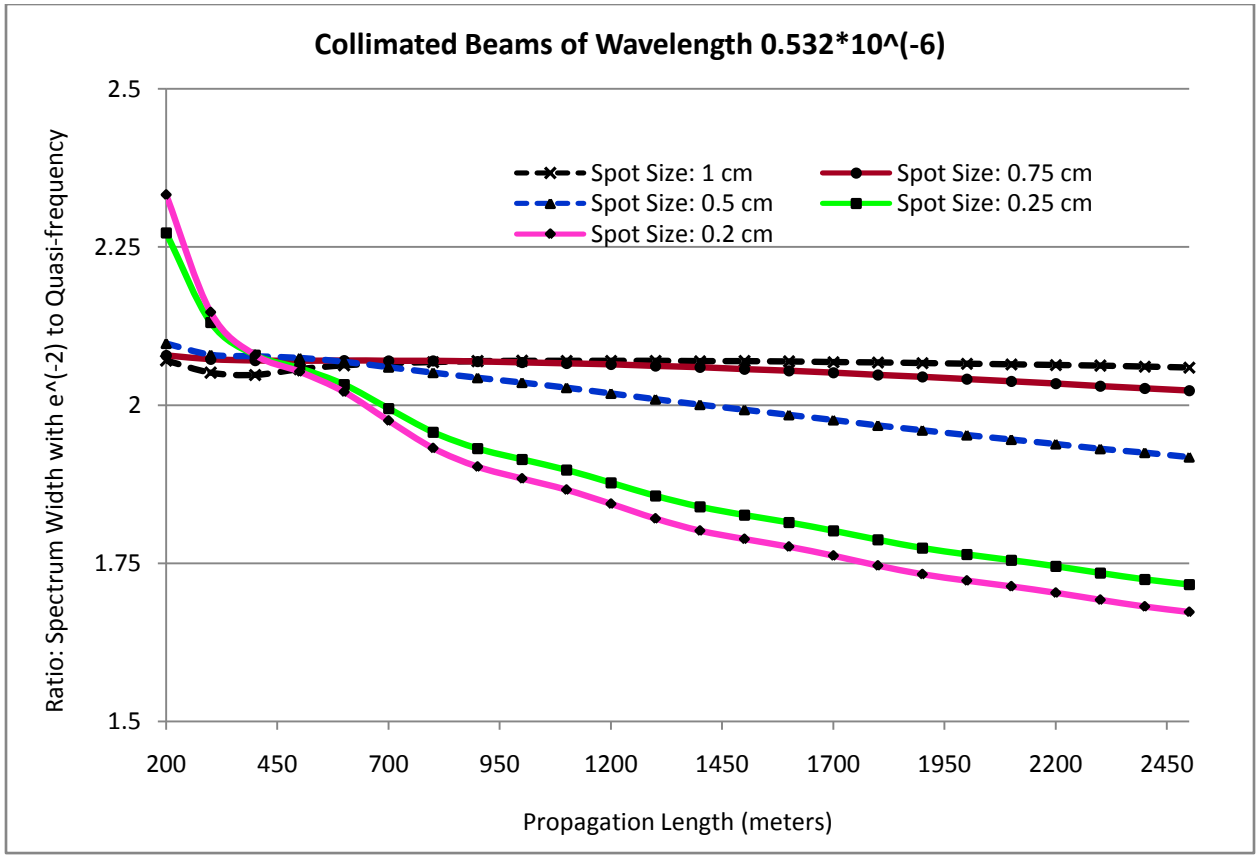

Figure 20: Ratio defined by the width of the $\hat{S}_{I,l}(\omega)$ using constant e^{-2} scaled by the quasi-frequency. The ratio is a function of propagation length, *L*, for collimated beams with spot sizes 0.2 cm to 1 cm of wavelengths of 0.532×10^{-6} and transverse velocity is $V_{\perp}=5\,{}^{m}\!/_{s}$.

Based on the data provided in Figures 17, 18, 19, and 20, comparing the spectrum width using the constant e^{-2} to the quasi-frequency, the spectral width is roughly $1\frac{3}{4}v_0$ to $2v_0$.

Note that calculating the quasi-frequency using (56) required the use of numerical methods over a finite interval. Instead of integrating the temporal spectrum (45) to calculate the quasi-frequency given by (56), recall that the quasi-frequency was originally defined by (53).Using (53), we can express the quasi-frequency for on-axis beam irradiance for collimated beams as, see appendix H,

$$\nu_0 = \frac{1}{2\pi}\left[-\frac{5V_\perp^2 k\left\{\Lambda^{1/6} d_3^{1/6}\left[(\Lambda d_3)^2 + (1-\overline{\Theta} d_3)^2\right]^{-1/12}\cos\left[\frac{1}{6}\tan^{-1}\left(\frac{1-\overline{\Theta} d_3}{\Lambda d_3}\right)\right]-1\right\}}{12 L d_3^{7/6}\Lambda^{1/6}\left[(\Lambda d_3)^2 + (1-\overline{\Theta} d_3)^2\right]^{5/12}\cos\left[\frac{5}{6}\tan^{-1}\left(\frac{1-\overline{\Theta} d_3}{\Lambda d_3}\right)\right] - \Lambda d_3^{5/6}}\right]^{1/2}, \qquad 60$$

where $d_3 = 0.67 - 0.17\Theta$. Recall that for plane and spherical waves, both have the parameter $\Lambda = 0$, which implies that (60) is not valid for plane and spherical wave cases. The interesting quality about the quasi-frequency defined by (60) is that the quasi-frequency can be expressed in terms of beam parameters for collimated beams. The values for the quasi-frequency calculated using (56) are equivalent to the values generated by (60)

CONCLUSIONS

The extended random medium model describes most optical wave propagation environments over a horizontal path. However, the integration associated with the extended model has not yet led to analytic expressions for some beam characteristics, like the covariance function of irradiance fluctuations. Using Andrews' thin random phase screen model allows for mathematical simplifications that do lead to approximate analytic expressions for beam characteristics. We have derived expressions for the scintillation index, covariance function of irradiance fluctuations, and the temporal spectrum of irradiance fluctuations for a thin phase screen model. Treating the normalized temporal spectrum of irradiance fluctuations as a probability density function allows the use of statistical tools to describe characteristics about the spectrum. We found that the quasi-frequency for on-axis points of a beam gives an approximation for the spectrum width. It has been shown that the width, using the Fresnel frequency, of the on-axis temporal spectrum can be approximated by three quarters of the quasi-frequency. From another perspective, when computing fade statistics we now have a reasonable approximation for the quasi-frequency expressed in terms of the Fresnel frequency. Finally, we have shown that the width, using the constant e^{-2}, of the on-axis temporal spectrum can be approximated by twice the quasi-frequency

APPENDIX A: INTEGRALS, PROPERTIES, AND ASYMPTOTIC FORMS

Most of the following integrals, properties, and asymptotic forms were used throughout this paper. [8]

A 1 $$\int_0^\infty e^{-st}t^{x-1}dt = \frac{\Gamma(x)}{s^x}, \text{ for } x>0 \text{ and } s>0.$$

A 2 $$\int_0^\infty x^\mu \exp\left(-a^2x^2\right)J_p(bx)dx = \frac{b^p\Gamma\left(\frac{p+\mu+1}{2}\right)}{2^{p+1}a^{p+\mu+1}\Gamma(p+1)}{}_1F_1\left(\frac{p+\mu+1}{2};p+1;-\frac{b^2}{4a^2}\right),$$

for $\mathrm{Re}(\mu+p)>-1$ and $a,b>0.$

A 3 $$\int_0^\infty x^{2\mu-1}\exp\left(-a^2x^2\right)J_0(bx)dx = \frac{1}{2a^{2\mu}}\Gamma(\mu){}_1F_1\left(\mu;1;-\frac{b^2}{4a^2}\right),$$

for $a\geq 0,$ b > 0, and $\mu\neq 0,-1,-2,-3,...$

A 4 $$\int_0^\infty \mathrm{K}^{2\mu}\frac{\exp\left(-\mathrm{K}^2/\mathrm{K}_m^2\right)}{\left(\mathrm{K}_0^2+\mathrm{K}^2\right)^{11/6}}d\mathrm{K} = \frac{1}{2}\mathrm{K}_0^{2\mu-8/3}\Gamma\left(\mu+\frac{1}{2}\right)U\left(\mu+\frac{1}{2};\mu-\frac{1}{3};\frac{\mathrm{K}_0^2}{\mathrm{K}_m^2}\right), \text{ for } \mu>-\frac{1}{2}.$$

The generalized hypergeometric function has the series representation

A 5 $${}_pF_q(a_1,...,a_p;c_1,...,c_q;z) = \sum_{n=0}^\infty \frac{(a_1)_n...(a_p)_n}{(c_1)_n...(c_q)_n}\frac{x^n}{n!},$$ where *p* and *q* are nonnegative integers and no c_k (k = 1, 2,…,q) is zero or a negative integer.

The Meijer G function has the series representation

A 6 $$G_{p,q}^{m,n}\left(x \left| \begin{matrix} a_1, & ..., & a_p \\ c_1, & ..., & c_q \end{matrix} \right. \right) = \sum_{k=1}^{m} \frac{\prod_{j=1}^{m}{}' \Gamma(c_j - c_k) \prod_{j=1}^{n} \Gamma(1 + c_k - a_j) x^{c_k}}{\prod_{j=m+1}^{q} \Gamma(1 + c_k - c_j) \prod_{j=n+1}^{p} \Gamma(a_j - c_k)}$$
$$\times {}_pF_{q-1}\left[1 + c_k - a_1, ..., 1 + c_k - a_p; 1 + c_k - c_1, ..., *, ..., 1 + c_k - c_q; (-1)^{p-m-n} x\right],$$

where $1 \le m \le q$, $0 \le n \le p \le q - 1$, no two of the c_k's ($k = 1,2,\ldots,m$) differ by zero or an integer, and $a_j - c_k \neq 1,2,3,\ldots$ for $j = 1,2,\ldots,n$ and $k = 1,2,\ldots,m$. If $p = q$, we restrict $|x| < 1$.

A 7 $$ {}_pF_q(a_1,...,a_p; c_1,...,c_q; x) = \frac{\prod_{j=1}^{q} \Gamma(c_j)}{\prod_{j=1}^{p} \Gamma(a_j)} G_{p,q+1}^{1,p}\left(-x \left| \begin{matrix} 1 - a_1, & ..., & 1 - a_p \\ 0, 1 - c_1, & ..., & 1 - c_q \end{matrix} \right. \right).$$

A 8 $$ {}_pF_q(a_1,...,a_p; c_1,...,c_q; x) = \frac{\prod_{j=1}^{q} \Gamma(c_j)}{\prod_{j=1}^{p} \Gamma(a_j)} G_{q+1,p}^{p,1}\left(-\frac{1}{x} \left| \begin{matrix} 1, c_1, & ..., & c_q \\ a_1, & ..., & a_p \end{matrix} \right. \right).$$

A 9 $$(a)_n = a(a+1)...(a+n-1) = \frac{\Gamma(a+n)}{\Gamma(a)},$$ for n = 1, 2, 3, …

A 10 $$(1)_n = n!.$$

A 11 $$\Gamma(x+1) = x\Gamma(x).$$

A 12 $$\Gamma(2n+1) = (2n)! = 2^{2n}\left(\frac{1}{2}\right)_n n!.$$

A 13 $${}_1F_1(a;c;z) \approx 1 - \frac{az}{c}, \text{ for } |z| << 1.$$

A 14 $${}_1F_1(a;c;z) \approx \frac{\Gamma(c)}{\Gamma(c-a)} z^{-a}, \text{ for } \mathrm{Re}|z| >> 1.$$

A 15 $${}_1F_0(a;-;z) = (1-a)^{-a}.$$

The Bessel function of the first kind has the series representation

A 16 $$J_p(z) = \sum_{n=0}^{\infty} \frac{(-1)^k}{k!\Gamma(k+p+1)} \left(\frac{z}{2}\right)^{2k+p}, \text{ for } |z| < \infty,$$

where *p* denotes the order of the function.

The modified Bessel functions of the first kind are defined by

A 17 $$I_p(z) = \sum_{n=0}^{\infty} \frac{1}{k!\Gamma(k+p+1)} \left(\frac{z}{2}\right)^{2k+p}, \text{ for } |z| < \infty,$$

where *p* denotes the order of the function.

A 18 $$\mathrm{Re}\left[J_0\left(\left|\vec{Q}\right|\right)\right] = J_0(x)I_0(y) + 2\sum_{n=1}^{\infty}(-1)^n J_{2n}(x)I_{2n}(y)\cos(2n\varphi),$$

where $\vec{Q} = \vec{x} - i\vec{y}$ and φ is the angle between $\vec{x}$ and $\vec{y}$.

APPENDIX B: SCINTILLATION INDEX

Assuming statistical homogeneity and isotropy and weak turbulence theory the scintillation is given as

$$\sigma_I^2(\vec{r},L)=8\pi^2k^2L\int_0^1\int_0^\infty \kappa\Phi_n(\kappa)\exp\left[-\frac{\Lambda L\kappa^2\xi^2}{k}\right]\left\{I_0(2\Lambda r\kappa\xi)-\cos\left[\frac{L\kappa^2}{k}\xi\left(1-\overline{\Theta}\xi\right)\right]\right\}d\kappa d\xi$$

Using the random thin phase screen model, take $d_2 << 1$ so that $1+d_2\eta\approx 1$, where $0\le\eta\le 1$,

$$\hat{\sigma}_I^2(\vec{r},L)=8\pi^2k^2Ld_2d_3\int_0^\infty \kappa\Phi_n(\kappa)\exp\left[-\frac{\Lambda L\kappa^2d_3^2}{k}\right]\left\{I_0(2\Lambda r\kappa d_3)-\cos\left[\frac{L\kappa^2}{k}d_3\left(1-\overline{\Theta}d_3\right)\right]\right\}d\kappa,$$

$$=8\pi^2k^2Ld_2d_3\int_0^\infty \kappa\Phi_n(\kappa)\exp\left[-\frac{\Lambda L\kappa^2d_3^2}{k}\right]\left\{I_0(2\Lambda r\kappa d_3)-1+1-\cos\left[\frac{L\kappa^2}{k}d_3\left(1-\overline{\Theta}d_3\right)\right]\right\}d\kappa,$$

$$=8\pi^2k^2Ld_2d_3\int_0^\infty \kappa\Phi_n(\kappa)\exp\left[-\frac{\Lambda L\kappa^2d_3^2}{k}\right]\left\{I_0(2\Lambda r\kappa d_3)-1\right\}d\kappa$$
$$+8\pi^2k^2Ld_2d_3\int_0^\infty \kappa\Phi_n(K)\exp\left[-\frac{\Lambda L\kappa^2d_3^2}{k}\right]\left\{1-\cos\left[\frac{L\kappa^2}{k}d_3\left(1-\overline{\Theta}d_3\right)\right]\right\}d\kappa.$$

The radial component of the scintillation index is identified as

$$\hat{\sigma}_{I,r}^2(\vec{r},L)=8\pi^2k^2Ld_2d_3\int_0^\infty \kappa\Phi_n(\kappa)\exp\left[-\frac{\Lambda L\kappa^2d_3^2}{k}\right]\left\{I_0(2\Lambda r\kappa d_3)-1\right\}d\kappa, \qquad \text{B 1}$$

and the longitudinal component of the scintillation index is identified as

$$\hat{\sigma}_{I,l}^2(\vec{r},L)=8\pi^2k^2Ld_2d_3\int_0^\infty \kappa\Phi_n(\kappa)\exp\left[-\frac{\Lambda L\kappa^2d_3^2}{k}\right]\left\{1-\cos\left[\frac{L\kappa^2}{k}d_3\left(1-\overline{\Theta}d_3\right)\right]\right\}d\kappa. \qquad \text{B 2}$$

For the radial component of the scintillation index, let's use the Kolmogorov spectrum $\Phi_n(\kappa) = 0.033\hat{C}_n^2\kappa^{-11/3}$, where $\hat{C}_n^2$ is the refractive-index structure constant for the phase screen, and the Maclaurin series representation $I_0(2\Lambda\kappa r d_3) - 1 = \sum_{n=1}^{\infty} \frac{(\Lambda r)^{2n}}{(n!)^2}\kappa^{2n} d_3^{2n}$, thus (B1) becomes

$$\hat{\sigma}_{I,r}^2(\vec{r}, L) = 8(0.033)\pi^2\hat{C}_n^2 k^2 L d_2 d_3 \int_0^{\infty} \kappa^{-8/3} \exp\left[-\frac{\Lambda L\kappa^2 d_3^2}{k}\right] \sum_{n=1}^{\infty} \frac{(\Lambda r)^{2n}}{(n!)^2}\kappa^{2n} d_3^{2n} d\kappa.$$

Assuming term-wise integration is permitted, then

$$\hat{\sigma}_{I,r}^2(\vec{r}, L) = 8(0.033)\pi^2\hat{C}_n^2 k^2 L d_2 d_3 \sum_{n=1}^{\infty} \frac{(\Lambda r)^{2n}}{(n!)^2} d_3^{2n} \int_0^{\infty} \kappa^{2n-8/3} \exp\left[-\frac{\Lambda L\kappa^2 d_3^2}{k}\right] d\kappa.$$

By making a change of variable of integration $t = K^2$ and using integral A1, in appendix A, we have

$$\hat{\sigma}_{I,r}^2(\vec{r}, L) = 8(0.033)\pi^2\hat{C}_n^2 k^2 L d_2 d_3 \sum_{n=1}^{\infty} \frac{(\Lambda r)^{2n}}{(n!)^2} d_3^{2n} \frac{1}{2}\Gamma\left(n - \frac{5}{6}\right)\left(\frac{\Lambda L}{k}\right)^{5/6 - n} d_3^{5/3 - 2n}.$$

Using properties A9, A10, and A11, in appendix A, then

$$\hat{\sigma}_{I,r}^2(\vec{r}, L) = 4(0.033)\left(-\frac{6}{5}\right)\Gamma\left(\frac{1}{6}\right)\pi^2\hat{C}_n^2 k^{7/6} L^{11/6} d_2 d_3^{8/3} \Lambda^{5/6} \sum_{n=1}^{\infty} \frac{\left(-\frac{5}{6}\right)_n}{(1)_n\, n!}\left(\frac{\Lambda k}{L} r^2\right)^n,$$

$$= 4(0.033)\left(-\frac{6}{5}\right)\Gamma\left(\frac{1}{6}\right)\pi^2\hat{C}_n^2 k^{7/6} L^{11/6} d_2 d_3^{8/3} \Lambda^{5/6}\left[\sum_{n=1}^{\infty} \frac{\left(-\frac{5}{6}\right)_n}{(1)_n\, n!}\left(\frac{\Lambda k}{L} r^2\right)^n + 1 - 1\right].$$

Using the definition of the generalized hypergeometric function, A5, we obtain

$$\hat{\sigma}_{I,r}^2(\vec{r},L)=8.70207\hat{C}_n^2k^{7/6}L^{11/6}d_2d_3^{11/6}(\Lambda d_3)^{5/6}\left[1-{}_1F_1\left(-\frac{5}{6};1;\frac{\Lambda k}{L}r^2\right)\right].$$

We can approximate the radial component of the scintillation index by recalling (5), $\Lambda=\frac{2L}{kW^2}$, then

$$\hat{\sigma}_{I,r}^2(\vec{r},L)=8.70207\hat{C}_n^2k^{7/6}L^{11/6}d_2d_3^{11/6}(\Lambda d_3)^{5/6}\left[1-{}_1F_1\left(-\frac{5}{6};1;\frac{2r^2}{W^2}\right)\right].$$

By taking $r<W$, which implies that $\frac{r^2}{W^2}<<1$ and applying asymptotic form, A13, in appendix A, we have

$$\hat{\sigma}_{I,r}^2(\vec{r},L)=8.70207\hat{C}_n^2k^{7/6}L^{11/6}d_2d_3^{11/6}(\Lambda d_3)^{5/6}\left[1-\left(1-\frac{5r^2}{3W^2}\right)\right].$$

Recall that $\hat{\sigma}_R^2=2.25\hat{C}_n^2L^{11/6}d_2d_3^{11/6}$, then the radial component of the scintillation index simplifies to

$$\hat{\sigma}_{I,r}^2(\vec{r},L)=6.45\hat{\sigma}_R^2(\Lambda d_3)^{5/6}\frac{r^2}{W^2}. \qquad \text{B 3}$$

For the longitudinal component of the scintillation index, let's use the Kolmogorov spectrum $\Phi_n(K)=0.033\hat{C}_n^2K^{-11/3}$ (where $\hat{C}_n^2$ is the refractive-index structure constant for the phase screen), and recall that $\mathrm{Re}\left(e^{i\vartheta}\right)=\cos\vartheta$,

$$\hat{\sigma}_{I,l}^2(\vec{r},L)=8(0.033)\pi^2\hat{C}_n^2k^2Ld_2d_3\int_0^\infty\kappa^{-8/3}\exp\left[-\frac{\Lambda L\kappa^2d_3^2}{k}\right]\mathrm{Re}\left\{1-\exp\left[i\frac{L\kappa^2}{k}d_3\left(1-\overline{\Theta}d_3\right)\right]\right\}d\kappa.$$

Let's expand the complex exponent in its series from, which leads to

$$\hat{\sigma}_{I,l}^2(\vec{r},L)=8(0.033)\pi^2\hat{C}_n^2k^2Ld_2d_3\int_0^\infty\kappa^{-8/3}\exp\left[-\frac{\Lambda L\kappa^2d_3^2}{k}\right]\mathrm{Re}\left\{1-\sum_{m=0}^{\infty}\frac{1}{m!}\left(\frac{iLd_3}{k}\right)^m\left(1-\overline{\Theta}d_3\right)^m\kappa^{2m}\right\}d\kappa.$$

Assuming term-wise integration is permitted, then

$$\hat{\sigma}_{I,l}^2(\vec{r},L)=-8(0.033)\pi^2\hat{C}_n^2Ld_2d_3\,\mathrm{Re}\left\{\sum_{m=1}^{\infty}\frac{1}{m!}\left(\frac{iLd_3}{k}\right)^m\left(1-\overline{\Theta}d_3\right)^m\int_0^\infty\kappa^{2m-8/3}\exp\left(-\frac{\Lambda Ld_3^2}{k}\kappa^2\right)d\kappa\right\}.$$

Using integral A1, in appendix A, we have

$$\hat{\sigma}_{I,l}^2(\vec{r},L)=-8(0.033)\pi^2\hat{C}_n^2Ld_2d_3\,\mathrm{Re}\left\{\sum_{m=1}^{\infty}\frac{1}{m!}\left(\frac{iLd_3}{k}\right)^m\left(1-\overline{\Theta}d_3\right)^m\frac{1}{2}\Gamma\left(m-\frac{5}{6}\right)\left(\frac{\Lambda Ld_3^2}{k}\right)^{5/6-m}\right\}.$$

Using property A11, in appendix A, we obtain

$$\hat{\sigma}_{I,l}^2(\vec{r},L)=-4(0.033)\left(-\frac{6}{5}\right)\Gamma\left(\frac{1}{6}\right)\pi^2\hat{C}_n^2k^{7/6}L^{11/6}d_2d_3^{8/3}\Lambda^{5/6}\,\mathrm{Re}\left\{\sum_{m=1}^{\infty}\left(-\frac{5}{6}\right)_m\frac{1}{m!}\left[\frac{i\left(1-\overline{\Theta}d_3\right)}{\Lambda d_3}\right]^m\right\},$$

$$=-4(0.033)\left(-\frac{6}{5}\right)\Gamma\left(\frac{1}{6}\right)\pi^2\hat{C}_n^2k^{7/6}L^{11/6}d_2d_3^{8/3}\Lambda^{5/6}\,\mathrm{Re}\left\{\sum_{m=1}^{\infty}\left(-\frac{5}{6}\right)_m\frac{1}{m!}\left[\frac{i\left(1-\overline{\Theta}d_3\right)}{\Lambda d_3}\right]^m+1-1\right\}.$$

Using the definition of the hypergeometric function, we have

$$\hat{\sigma}_{I,l}^2(\vec{r},L)=8.70207\hat{C}_n^2k^{7/6}L^{11/6}d_2d_3^{11/6}(\Lambda d_3)^{5/6}\,\mathrm{Re}\left\{{}_1F_0\left(-\frac{5}{6};-;\frac{i\left[1-\overline{\Theta}d_3\right]}{\Lambda d_3}\right)-1\right\}.$$

Using property A12, in appendix A, we have

$$\hat{\sigma}_{I,l}^2(\vec{r},L)=8.70207\hat{C}_n^2k^{7/6}L^{11/6}d_2d_3^{11/6}(\Lambda d_3)^{5/6}\,\mathrm{Re}\left\{\left(1-\frac{i\left[1-\overline{\Theta}d_3\right]}{\Lambda d_3}\right)^{5/6}-1\right\}.$$

Using (G1) from appendix G, we have $\alpha=\frac{5}{6}$ and it follows that

$$\hat{\sigma}_{I,l}^2(\vec{r},L)=8.70207\hat{C}_n^2k^{7/6}L^{11/6}d_2d_3^{11/6}(\Lambda d_3)^{5/6}\left\{(\Lambda d_3)^{-5/6}\left[(\Lambda d_3)^2+(1-\overline{\Theta}d_3)^2\right]^{5/12}\right.$$
$$\left.\times\cos\left[\frac{5}{6}\tan^{-1}\left(\frac{1-\overline{\Theta}d_3}{\Lambda d_3}\right)\right]-1\right\}.$$

Recall that $\hat{\sigma}_R^2=2.25\hat{C}_n^2L^{11/6}d_2d_3^{11/6}$, then the longitudinal component of the scintillation index simplifies to

$$\hat{\sigma}_{I,l}^2(\vec{r},L)=3.87\hat{\sigma}_R^2\left\{\left[(\Lambda d_3)^2+(1-\overline{\Theta}d_3)^2\right]^{5/12}\cos\left[\frac{5}{6}\tan^{-1}\left(\frac{1-\overline{\Theta}d_3}{\Lambda d_3}\right)\right]-(\Lambda d_3)^{5/6}\right\}. \qquad \text{B 4}$$

By combining the radial and longitudinal components, (B3) and (B4), we have the total scintillation index using the random thin phase screen model, where $r<W$

$$\hat{\sigma}_R^2(\vec{r},L)\cong 6.45\hat{\sigma}_R^2(\Lambda d_3)^{5/6}\frac{r^2}{W^2}+3.87\hat{\sigma}_R^2\left\{\left[(\Lambda d_3)^2+(1-\overline{\Theta}d_3)^2\right]^{5/12}\right.$$
$$\left.\times\cos\left[\frac{5}{6}\tan^{-1}\left(\frac{1-\overline{\Theta}d_3}{\Lambda d_3}\right)\right]-(\Lambda d_3)^{5/6}\right\}. \qquad \text{B 5}$$

APPENDIX C: COVARIANCE FUNCTION UNDER THE FROZEN TURBULENCE HYPOTHESIS

Assuming weak turbulence theory and statistical homogeneity and isotropy, for two points in the beam $\vec{r}_1$ and $\vec{r}_2$ the covariance is defined as:

$$B_I(\vec{p},\vec{r},L) = 8\pi^2 k^2 L \int_0^1 \int_0^\infty \kappa \Phi_n(\kappa) \exp\left(-\frac{\Lambda L \xi^2 \kappa^2}{k}\right) \mathrm{Re}\left\{ J_0\left[\kappa\left|\left(1-\overline{\Theta}\xi\right)\vec{p} - 2i\Lambda\xi\vec{r}\right|\right] - \exp\left[-\frac{iL\kappa^2}{k}\xi\left(1-\overline{\Theta}\xi\right)\right] J_0\left[\left(1-\overline{\Theta}\xi - i\Lambda\xi\right)\rho\kappa\right]\right\} d\kappa d\xi,$$

where $\vec{r} = \frac{1}{2}(\vec{r}_1 + \vec{r}_2)$, $\vec{p} = \vec{r}_1 - \vec{r}_2$, $\rho = |\vec{p}|$, and the normalized distance for $0 \le z \le L$ is given as $\xi = 1 - \frac{z}{L}$, so that $0 \le \xi \le 1$. In addition, the absolute value in the Bessel function refers to the magnitude of the vector expression, not the complex expression. The path amplitude ratio is defined as:

$$\gamma = 1 - \left(\overline{\Theta} + i\Lambda\right)\xi = \left(1 - \overline{\Theta}\xi\right) - i\Lambda\xi \quad \text{and} \quad \gamma^* = \left(1 - \overline{\Theta}\xi\right) + i\Lambda\xi.$$

Using the path amplitude ratio, the covariance function becomes

$$B_I(\vec{p},\vec{r},L) = 8\pi^2 k^2 L \int_0^1 \int_0^\infty \kappa \Phi_n(\kappa) \exp\left(-\frac{\Lambda L \xi^2 \kappa^2}{k}\right) \mathrm{Re}\left\{ J_0\left[\kappa\left|\frac{\gamma\vec{p}}{2} + \frac{\gamma^*\vec{p}}{2} + \gamma\vec{r} - \gamma^*\vec{r}\right|\right] - \exp\left[-\frac{iL\kappa^2}{k}\xi\left(1-\overline{\Theta}\xi\right)\right] J_0\left[\gamma\rho\kappa\right]\right\} d\kappa d\xi.$$

The frozen turbulence hypothesis dictates that we replace $\gamma\,\vec{p} = \vec{V}_\perp \vec{\tau}$ and $\gamma^*\vec{p} = \vec{V}_\perp \vec{\tau}$, thus

$$B_I(\tau,r,L)=8\pi^2k^2L\int_0^1\int_0^\infty \kappa\Phi_n(\kappa)\exp\left(-\frac{\Lambda L\xi^2\kappa^2}{k}\right)\mathrm{Re}\left\{J_0\left[\left|\kappa\vec{V}_\perp\vec{\tau}-i2\Lambda\kappa\xi\vec{r}\right|\right]\right.$$
$$\left.-\exp\left[-\frac{iL\kappa^2}{k}\xi\left(1-\overline{\Theta}\xi\right)\right]J_0\left[\kappa V_\perp\tau\right]\right\}d\kappa d\xi,$$

where $V_\perp\tau=\left|\vec{V}_\perp\vec{\tau}\right|$ and $r=\left|\vec{r}\right|$. We can approximate the covariance function by taking the first term of the series representation of $J_0\left[\left|\kappa\vec{V}_\perp\vec{\tau}-i2\Lambda\kappa\xi\vec{r}\right|\right]$, using property A18, in appendix A, thus

$$B_I(\tau,r,L)=8\pi^2k^2L\int_0^1\int_0^\infty \kappa\Phi_n(\kappa)\exp\left(-\frac{\Lambda L\xi^2\kappa^2}{k}\right)\mathrm{Re}\left\{J_0\left[\kappa V_\perp\tau\right]\left(I_0\left[2\Lambda\kappa\xi r\right]\right.\right.$$
$$\left.\left.-\exp\left[-\frac{iL\kappa^2}{k}\xi\left(1-\overline{\Theta}\xi\right)\right]\right)\right\}d\kappa d\xi.$$

Let's separate the covariance function into the sum of two integrals,

$$B_I(\tau,r,L)=8\pi^2k^2L\int_0^1\int_0^\infty \kappa\Phi_n(\kappa)\exp\left(-\frac{\Lambda L\xi^2\kappa^2}{k}\right)\mathrm{Re}\left\{J_0\left[\kappa V_\perp\tau\right]\left(I_0\left[2\Lambda\kappa\xi r\right]+1-1\right.\right.$$
$$\left.\left.-\exp\left[-\frac{iL\kappa^2}{k}\xi\left(1-\overline{\Theta}\xi\right)\right]\right)\right\}d\kappa d\xi,$$

$$=8\pi^2k^2L\int_0^1\int_0^\infty \kappa\Phi_n(\kappa)\exp\left(-\frac{\Lambda L\xi^2\kappa^2}{k}\right)J_0\left[\kappa V_\perp\tau\right]\left(I_0\left[2\Lambda\kappa\xi r\right]-1\right)d\kappa d\xi$$
$$+8\pi^2k^2L\int_0^1\int_0^\infty \kappa\Phi_n(\kappa)\exp\left(-\frac{\Lambda L\xi^2\kappa^2}{k}\right)\mathrm{Re}\left\{J_0\left[\kappa V_\perp\tau\right]\left(1-\exp\left[-\frac{iL\kappa^2}{k}\xi\left(1-\overline{\Theta}\xi\right)\right]\right)\right\}d\kappa d\xi.$$

Now we can identify the radial and longitudinal components of the covariance function, the radial component is

$$B_{I,r}(\tau,r,L)=8\pi^2k^2L\int_0^1\int_0^\infty \kappa\Phi_n(\kappa)\exp\left(-\frac{\Lambda L\xi^2\kappa^2}{k}\right)J_0\left[\kappa V_\perp\tau\right]\left(I_0\left[2\Lambda\kappa\xi r\right]-1\right)d\kappa d\xi\,, \qquad \text{C 1}$$

and the longitudinal component is

$$B_{I,l}(\tau,r,L)=8\pi^2k^2L\int_0^1\int_0^\infty \kappa\Phi_n(\kappa)\exp\left(-\frac{\Lambda L\xi^2\kappa^2}{k}\right)\mathrm{Re}\left\{J_0\left[\kappa V_\perp\tau\right]\right.$$
$$\left.\times\left(1-\exp\left[-\frac{iL\kappa^2}{k}\xi\left(1-\overline{\Theta}\xi\right)\right]\right)\right\}d\kappa d\xi\,. \qquad \text{C 2}$$

APPENDIX D: TEMPORAL COVARIANCE FUNCTION

Assuming weak turbulence theory and statistical homogeneity and isotropy, the covariance function under the frozen turbulence hypothesis, from appendix C, is given as:

$$B_I(\tau,r,L)=8\pi^2k^2L\int_0^1\int_0^\infty \kappa\Phi_n(\kappa)\exp\left(-\frac{\Lambda L\xi^2\kappa^2}{k}\right)\mathrm{Re}\left\{J_0(\kappa V_\perp\tau)\left(I_0[2\Lambda\kappa\xi r]\right.\right.$$
$$\left.\left.-\exp\left[-\frac{iL\kappa^2}{k}\xi(1-\overline{\Theta}\xi)\right]\right)\right\}d\kappa d\xi\,.$$

Separating the covariance function into its radial and longitudinal components, we have

$$B_{I,r}(\tau,r,L)=8\pi^2k^2L\int_0^1\int_0^\infty \kappa\Phi_n(\kappa)\exp\left(-\frac{\Lambda L\xi^2\kappa^2}{k}\right)J_0(\kappa V_\perp\tau)(I_0[2\Lambda\kappa\xi r]-1)d\kappa d\xi\,, \qquad \text{D 1}$$

and

$$B_{I,l}(\tau,r,L)=8\pi^2k^2L\int_0^1\int_0^\infty \kappa\Phi_n(\kappa)\exp\left(-\frac{\Lambda L\xi^2\kappa^2}{k}\right)\mathrm{Re}\left\{J_0[\kappa V_\perp\tau]\right.$$
$$\left.\times\left(1-\exp\left[-\frac{iL\kappa^2}{k}\xi(1-\overline{\Theta}\xi)\right]\right)\right\}d\kappa d\xi\,. \qquad \text{D 2}$$

Let's assume weak turbulence theory, and use the Kolmogorov spectrum $\Phi_n(K)=0.033\hat{C}_n^2\kappa^{-11/3}$ to calculate the covariance function. In addition, let's use the random thin phase screen model and take $d_2<<1$, so that $1+d_2\eta\approx 1$ where $0\le\eta\le 1$. Then radial component (D1) under the above conditions becomes

$$B_{I,r}(\tau,r,L)=8(0.033)\pi^2\hat{C}_n^2k^2Ld_2d_3\int_0^\infty \kappa^{-8/3}\exp\left(-\frac{\Lambda Ld_3^2\kappa^2}{k}\right)J_0(\kappa V_\perp\tau)(I_0[2\Lambda\kappa d_3 r]-1)d\kappa\,.$$

Using the Maclaurin series representation $I_0(2\Lambda\kappa r d_3)-1=\sum_{n=1}^{\infty}\frac{(\Lambda r)^{2n}}{(n!)^2}\kappa^{2n}d_3^{2n}$ and assuming term-wise integration is permitted, we have

$$B_{I,r}(\tau,r,L)=8(0.033)\pi^2\hat{C}_n^2k^2Ld_2d_3\sum_{n=1}^{\infty}\frac{(\Lambda r)^{2n}}{(n!)}d_3^{2n}\int_0^{\infty}\kappa^{2n-8/3}\exp\left(-\frac{\Lambda L d_3^2\kappa^2}{k}\right)J_0(\kappa V_\perp\tau)d\kappa.$$

Using integral A2, in appendix A, then

$$B_{I,r}(\tau,r,L)=8(0.033)\pi^2\hat{C}_n^2k^2Ld_2d_3\sum_{n=1}^{\infty}\frac{(\Lambda r)^{2n}}{(n!)^2}d_3^{2n}\frac{k^{n-5/6}\Gamma\left(n-\frac{5}{6}\right)}{2(\Lambda L)^{n-5/6}d_3^{2n-5/3}}{}_1F_1\left(n-\frac{5}{6};1;-\frac{V_\perp^2\tau^2k}{4\Lambda Ld_3^2}\right).$$

Note that weak turbulence theory suggests that $(\Lambda r)<<1$, thus we can approximate the series by using its first term, so we have

$$B_{I,r}(\tau,r,L)\cong 8(0.033)\pi^2\hat{C}_n^2k^2Ld_2d_3\bullet\frac{1}{2}\Gamma\left(\frac{1}{6}\right)r^2\left(\frac{L}{k}\right)^{-1/6}\Lambda^{11/6}d_3^{5/3}{}_1F_1\left(\frac{1}{6};1;-\frac{V_\perp^2\tau^2k}{4\Lambda Ld_3^2}\right). \qquad \text{D 3}$$

Recall from (5) that $\Lambda=\frac{2z}{kW^2}$, which implies that

$$\frac{1}{W^2}=\frac{k\Lambda}{2z}. \qquad \text{D 4}$$

Let's define the Fresnel frequency as $\omega_t=\frac{V_\perp}{\sqrt{L/k}}$ and it follows that

$$\omega_t^2=\frac{V_\perp^2k}{L}. \qquad \text{D 5}$$

By substituting (D4) and (D5) into (D3) and simplifying the expression, the radial component becomes

$$B_{I,r}(\tau,r,L)\cong 6.45\hat{\sigma}_R^2(\Lambda d_3)^{5/6}\left(\frac{r}{W}\right)^2{}_1F_1\left(\frac{1}{6};1;-\frac{\omega_t^2\tau^2}{4\Lambda d_3^2}\right), \qquad \text{D 6}$$

where $\hat{\sigma}_R^2=2.25\hat{C}_n^2L^{11/6}d_2d_3^{11/6}$, which is the Rytov variance for the thin phase screen model. As for the longitudinal component, notice that taking $\vec{r}=0$ does not change the expression on the right side of (D2). Thus the longitudinal component using the thin phase screen model can be written as

$$B_{I,l}(\tau,L)=8\pi^2k^2Ld_2d_3\int_0^\infty\kappa\Phi_n(\kappa)\exp\left(-\frac{\Lambda Ld_3^2\kappa^2}{k}\right)\mathrm{Re}\left\{J_0\left[\kappa V_\perp\tau\right]\left(1-\exp\left[-\frac{iL\kappa^2}{k}d_3\left(1-\overline{\Theta}d_3\right)\right]\right)\right\}d\kappa.$$

Using the Kolmogorov spectrum $\Phi_n(\kappa)=0.033\hat{C}_n^2\kappa^{-11/3}$ and separating the expression on the right into two integrals, we have

$$\begin{aligned}B_{I,l}(\tau,L)&=8(0.033)\pi^2\hat{C}_n^2k^2Ld_2d_3\,\mathrm{Re}\left\{\int_0^\infty\kappa^{-8/3}\exp\left(-\frac{\Lambda Ld_3^2}{k}\kappa^2\right)J_0(\kappa V_\perp\tau)d\kappa\right\}\\&\quad-8(0.033)\pi^2\hat{C}_n^2k^2Ld_2d_3\,\mathrm{Re}\left\{\int_0^\infty\kappa^{-8/3}\exp\left[-\kappa^2\frac{Ld_3}{k}\left(\Lambda d_3+i\left[1-\overline{\Theta}d_3\right]\right)\right]J_0(\kappa V_\perp\tau)d\kappa\right\},\\&=8(0.033)\pi^2\hat{C}_n^2k^2Ld_2d_3\int_0^\infty\kappa^{-8/3}\exp\left(-\frac{\Lambda Ld_3^2\kappa^2}{k}\right)J_0(\kappa V_\perp\tau)d\kappa\\&\quad-8(0.033)\pi^2\hat{C}_n^2k^2Ld_2d_3\int_0^\infty\kappa^{-8/3}\exp\left(-\frac{\Lambda Ld_3^2\kappa^2}{k}\right)\mathrm{Re}\left\{J_0(\kappa V_\perp\tau)\exp\left[-\frac{iL\kappa^2}{k}d_3\left(1-\overline{\Theta}d_3\right)\right]\right\}d\kappa.\end{aligned}$$

Let's define

$$X = 8(0.033)\pi^2 \hat{C}_n^2 k^2 L d_2 d_3 \int_0^\infty \kappa^{-8/3} \exp\left(-\frac{\Lambda L d_3^2 \kappa^2}{k}\right) J_0(\kappa V_\perp \tau) d\kappa,$$

and

$$Y = 8(0.033)\pi^2 \hat{C}_n^2 k^2 L d_2 d_3 \int_0^\infty \kappa^{-8/3} \exp\left(-\frac{\Lambda L d_3^2 \kappa^2}{k}\right) \mathrm{Re}\left\{ J_0(\kappa V_\perp \tau) \exp\left[-\frac{iL\kappa^2}{k} d_3 \left(1 - \overline{\Theta} d_3\right)\right]\right\} d\kappa.$$

so that $B_{I,l}(\tau, L) = X - Y$. To evaluate the integral *X*, let's use integral A3 in appendix A, then

$$X = 8(0.033)\pi^2 \hat{C}_n^2 k^2 L d_2 d_3 \frac{\Gamma\left(-\frac{5}{6}\right)\left(\Lambda L d_3^2\right)^{5/6}}{2k^{5/6}} {}_1F_1\left(-\frac{5}{6}; 1; -\frac{V_\perp^2 \tau^2 k}{4\Lambda L d_3^2}\right).$$

Simplifying and substituting (D5) into the right side, and recalling that $\hat{\sigma}_R^2 = 2.25 \hat{C}_n^2 L^{11/6} d_2 d_3^{11/6}$, gives us

$$X = -3.8637 \hat{\sigma}_R^2 \left(\Lambda d_3\right)^{5/6} {}_1F_1\left(-\frac{5}{6}; 1; -\frac{\omega_t^2 \tau^2}{4\Lambda d_3^2}\right). \qquad \text{D 7}$$

To evaluate the integral represented by Y, we once again apply property A3 in appendix A, thus

$$Y = 8(0.033)\pi^2 \hat{C}_n^2 k^2 L d_2 d_3 \,\mathrm{Re}\left\{ \frac{\Gamma\left(-\frac{5}{6}\right) k^{-5/6}}{2(L d_3)^{-5/6}\left(\Lambda d_3 + i\left[1-\overline{\Theta} d_3\right]\right)^{-5/6}} \right.$$

$$\left. \times {}_1F_1\left(-\frac{5}{6}; 1; -\frac{V_\perp^2 \tau^2 k}{4 L d_3 \left(\Lambda d_3 + i\left[1-\overline{\Theta} d_3\right]\right)} \right) \right\}.$$

Observe that $\left(\Lambda d_3 + i\left[1-\overline{\Theta} d_3\right]\right)^{5/6} = i^{5/6}\left[1-\left(\overline{\Theta}+i\Lambda\right)d_3\right]^{5/6}$. Simplifying and substituting (D5) into the right side and recalling that $\hat{\sigma}_R^2 = 2.25 \hat{C}_n^2 L^{11/6} d_2 d_3^{11/6}$, we have

$$Y = -3.8637 \hat{\sigma}_R^2 \,\mathrm{Re}\left\{ i^{5/6}\left[1-\left(\overline{\Theta}+i\Lambda\right)d_3\right]^{5/6} {}_1F_1\left(-\frac{5}{6}; 1; -\frac{\omega_\perp^2 \tau^2}{4 i d_3 \left[1-\left(\overline{\Theta}+i\Lambda\right)d_3\right]} \right) \right\}. \qquad \text{D 8}$$

By combining the results (D7) and (D8), the longitudinal component of the covariance function becomes $B_{I,l}(\tau, L) = X - Y$ and we have

$$B_{I,l}(\tau, L) = 3.8637 \hat{\sigma}_R^2 \,\mathrm{Re}\left\{ i^{5/6}\left[1-\left(\overline{\Theta}+i\Lambda\right)d_3\right]^{5/6} {}_1F_1\left(-\frac{5}{6}; 1; -\frac{\omega_\perp^2 \tau^2}{4 i d_3 \left[1-\left(\overline{\Theta}+i\Lambda\right)d_3\right]} \right) \right.$$

$$\left. -\left(\Lambda d_3\right)^{5/6} {}_1F_1\left(-\frac{5}{6}; 1; -\frac{\omega_t^2 \tau^2}{4 \Lambda d_3^2} \right) \right\}.$$

Let's define $a_1 = \dfrac{1}{4 d_3 i\left[1-\left(\overline{\Theta}+i\Lambda\right)d_3\right]}$ and $a_2 = \dfrac{1}{4\Lambda d_3^2}$, then the longitudinal component of the covariance function can be written as

$$B_{I,l}(\tau,L)=3.8637\hat{\sigma}_R^2\,\mathrm{Re}\left\{i^{5/6}\left[1-\left(\overline{\Theta}+i\Lambda\right)d_3\right]^{5/6}{}_1F_1\left(-\frac{5}{6};1;-a_1\omega_\perp^2\tau^2\right)\right.$$
$$\left.-\left(\Lambda d_3\right)^{5/6}{}_1F_1\left(-\frac{5}{6};1;-a_2\omega_t^2\tau^2\right)\right\}, \qquad \text{D 9}$$

where $d_3=0.67-0.17\Theta$. Combining the radial and longitudinal components, we have the total covariance function

$$B_I(\tau,r,L)\cong 6.45\hat{\sigma}_R^2\left(\Lambda d_3\right)^{5/6}\left(\frac{r^2}{W^2}\right){}_1F_1\left(\frac{1}{6};1;-a_2\omega_t^2\tau^2\right)$$
$$+3.8637\hat{\sigma}_R^2\,\mathrm{Re}\left\{i^{5/6}\left[1-\left(\overline{\Theta}+i\Lambda\right)d_3\right]^{5/6}{}_1F_1\left(-\frac{5}{6};1;-a_1\omega_t^2\tau^2\right)-\left(\Lambda d_3\right)^{5/6}{}_1F_1\left(-\frac{5}{6};1;-a_2\omega_t^2\tau^2\right)\right\}, \qquad \text{D 10}$$

or

$$B_I(\tau,r,L)\cong 6.45\hat{\sigma}_R^2\left(\Lambda d_3\right)^{5/6}\left(\frac{r^2}{W^2}\right){}_1F_1\left(\frac{1}{6};1;-a_2\omega_t^2\tau^2\right)$$
$$+3.8637\hat{\sigma}_R^2\,\mathrm{Re}\left\{\left[4a_1d_3\right]^{-5/6}{}_1F_1\left(-\frac{5}{6};1;-a_1\omega_t^2\tau^2\right)-\left(\Lambda d_3\right)^{5/6}{}_1F_1\left(-\frac{5}{6};1;-a_2\omega_t^2\tau^2\right)\right\}. \qquad \text{D 11}$$

APPENDIX E: POWER SPECTRAL DENSITY FUNCTION

The power spectral density (PSD), $S_I(\omega)$, is defined by the Fourier transform of the temporal covariance function by

$$S_I(\omega) = 2\int_{-\infty}^{\infty} B_I(\tau, L)\exp(-i\omega\tau)d\tau = 4\int_{0}^{\infty} B_I(\tau, L)\cos(\omega\tau)d\tau$$

where $B_I(\tau,L)$ is the temporal covariance function. The extra factor of 2 in the transform integral is a result of considering only positive frequencies. Due to the even property of the temporal covariance function with respect to τ and since the imaginary component of an even function is zero, we will use the real component of the complex exponential. Assuming weak turbulence theory and statistical homogeneity and isotropy, from appendix D, we know that

$$B_I(\tau,r,L) \cong 6.45\hat{\sigma}_R^2(\Lambda d_3)^{5/6}\left(\frac{r^2}{W^2}\right)_1F_1\left(\frac{1}{6};1;-\frac{\omega_t^2\tau^2}{4\Lambda d_3^2}\right)$$
$$+ 3.87\hat{\sigma}_R^2\,\mathrm{Re}\left\{[4a_1d_3]^{-5/6}{}_1F_1\left(-\frac{5}{6};1;-a_1\omega_t^2\tau^2\right) - (\Lambda d_3)^{5/6}{}_1F_1\left(-\frac{5}{6};1;-a_2\omega_t^2\tau^2\right)\right\},$$

which consists of the radial and longitudinal components

$$B_{I,r}(\tau,r,L) \cong 6.45\hat{\sigma}_R^2(\Lambda d_3)^{5/6}\left(\frac{r^2}{W^2}\right)_1F_1\left(\frac{1}{6};1;-\frac{\omega_t^2\tau^2}{4\Lambda d_3^2}\right),$$

and

$$B_{I,l}(\tau,L) = 3.87\hat{\sigma}_R^2\,\mathrm{Re}\left\{[4a_1d_3]^{-5/6}{}_1F_1\left(-\frac{5}{6};1;-a_1\omega_t^2\tau^2\right) - (\Lambda d_3)^{5/6}{}_1F_1\left(-\frac{5}{6};1;-a_2\omega_t^2\tau^2\right)\right\},$$

where $a_1 = \frac{1}{4d_3 i\left[1-\left(\overline{\Theta}+i\Lambda\right)d_3\right]}$, $a_2 = \frac{1}{4\Lambda d_3^2}$, and $\omega_t = \frac{V_\perp}{\sqrt{L/k}}$. Let's use the longitudinal component of the covariance function to calculate $S_{I,l}(\omega)$, then

$$S_{I,l}(\omega) = 4\int_0^\infty 3.87\hat{\sigma}_R^2 \,\mathrm{Re}\left\{\left[4a_1 d_3\right]^{-5/6} {}_1F_1\left(-\frac{5}{6};1;-a_1\omega_t^2\tau^2\right) - \left(\Lambda d_3\right)^{5/6} {}_1F_1\left(-\frac{5}{6};1;-a_2\omega_t^2\tau^2\right)\right\}\cos(\omega\tau)d\tau .$$

Integrating the difference of the two confluent hypergeometric functions converges, however the integration is a difficult task. Separating the single integral into a difference of two integrals gives

$$\begin{aligned} S_{I,l}(\omega) = {} & 4^{1/6}(3.87)\hat{\sigma}_R^2 d_3^{-5/6}\,\mathrm{Re}\left\{a_1^{-5/6}\int_0^\infty {}_1F_1\left(-\frac{5}{6};1;-a_1\omega_t^2\tau^2\right)\cos(\omega\tau)d\tau\right\} \\ & - 4(3.87)\hat{\sigma}_R^2\left(\Lambda d_3\right)^{5/6}\,\mathrm{Re}\left\{\int_0^\infty {}_1F_1\left(-\frac{5}{6};1;-a_2\omega_t^2\tau^2\right)\cos(\omega\tau)d\tau\right\}. \end{aligned}$$

It is important to note that each of the two integrals do not converge, yet their difference does converge. In order to integrate each integral, we need to use a mathematical tool to force convergence. Recall $\cos\vartheta = \frac{1}{2}\left(e^{i\vartheta}+e^{-i\vartheta}\right)$, then we can write $\cos(\omega\tau) = \frac{1}{2}\left(e^{i\omega\tau}+e^{-i\omega\tau}\right)$. Rather than replace the complex expression for cosine in the integrals, let's substitute the limiting case of $\cos(\omega\tau) = \frac{1}{2}\left(e^{i\omega\tau}+e^{-i\omega\tau}\right) = \frac{1}{2}\lim_{\alpha\to 0}\left(e^{-(\alpha+i\omega)\tau}+e^{-(\alpha-i\omega)\tau}\right)$ in the integrals. We have introduced the decaying exponent $e^{-\alpha}$ which will allow the integrals to converge. After the integration is complete, we will perform the limit as α approaches zero and obtain the result we desire. Let's split $S_{I,l}(\omega)$, into two integrals and take

$$X = 4^{1/6}(3.87)\hat{\sigma}_R^2 d_3^{-5/6}\ \mathrm{Re}\left\{a_1^{-5/6}\int_0^\infty {}_1F_1\left(-\frac{5}{6};1;-a_1\omega_t^2\tau^2\right)\cos(\omega\tau)d\tau\right\},$$

and

$$Y = 4(3.87)\hat{\sigma}_R^2(\Lambda d_3)^{5/6}\ \mathrm{Re}\left\{\int_0^\infty {}_1F_1\left(-\frac{5}{6};1;-a_2\omega_t^2\tau^2\right)\cos(\omega\tau)d\tau\right\},$$

so that $S_I(\omega) = X - Y$. Let's first integrate X. By substitute the limiting component into X, we have

$$X = \lim_{\alpha\to 0}\left(\frac{1}{2}4^{1/6}(3.87)\hat{\sigma}_R^2 d_3^{-5/6}\ \mathrm{Re}\left\{a_1^{-5/6}\left[\int_0^\infty {}_1F_1\left(-\frac{5}{6};1;-a_1\omega_t^2\tau^2\right)e^{-(\alpha+i\omega)\tau}d\tau\right.\right.\right.$$
$$\left.\left.\left.+\int_0^\infty {}_1F_1\left(-\frac{5}{6};1;-a_1\omega_t^2\tau^2\right)e^{-(\alpha-i\omega)\tau}\right]d\tau\right\}\right).$$

By writing the hypergeometric functions in their summation form, assuming term-wise integration is permitted, using integral A1 and property A12, in appendix A, we have

$$X = \lim_{\alpha\to 0}\left(\frac{1}{2}4^{1/6}(3.87)\hat{\sigma}_R^2 d_3^{-5/6}\ \mathrm{Re}\left\{a_1^{-5/6}\left[\frac{1}{\alpha+i\omega}{}_2F_0\left(-\frac{5}{6},\frac{1}{2};-\frac{4a_1\omega_t^2}{[\alpha+i\omega]^2}\right)\right.\right.\right.$$
$$\left.\left.\left.+\frac{1}{\alpha-i\omega}{}_2F_0\left(-\frac{5}{6},\frac{1}{2};-\frac{4a_1\omega_t^2}{[\alpha-i\omega]^2}\right)\right]\right\}\right).$$

After performing the limit operation, we have

$$X = \frac{1}{2}4^{1/6}(3.87)\hat{\sigma}_R^2 d_3^{-5/6}\ \mathrm{Re}\left\{a_1^{-5/6}\left[\frac{1}{(i\omega)}{}_2F_0\left(-\frac{5}{6},\frac{1}{2};-\frac{4a_1\omega_t^2}{[i\omega]^2}\right)+\frac{1}{(-i\omega)}{}_2F_0\left(-\frac{5}{6},\frac{1}{2};-\frac{4a_1\omega_t^2}{[-i\omega]^2}\right)\right]\right\}.$$

Let's transform the hypergeometric ${}_2F_0$ function into a linear combination of confluent hypergeometric functions, ${}_1F_1$, using (F2), in appendix F, we have

$$X = \frac{1}{2}4^{1/6}(3.87)\hat{\sigma}_R^2 d_3^{-5/6}\,\mathrm{Re}\left\{ a_1^{-5/6}\frac{1}{(i\omega)}\left[\frac{(i\omega)^2}{4a_1\omega_t^2}\right]^{-5/6}\left[\frac{\Gamma\left(\frac{4}{3}\right)}{\Gamma\left(\frac{1}{2}\right)}{}_1F_1\left(-\frac{5}{6};-\frac{1}{3};\frac{(i\omega)^2}{4a_1\omega_t^2}\right)\right.\right.$$
$$\left. + \frac{\Gamma\left(-\frac{4}{3}\right)}{\Gamma\left(-\frac{5}{6}\right)}\left[\frac{(i\omega)^2}{4a_1\omega_t^2}\right]^{4/3}{}_1F_1\left(\frac{1}{2};\frac{7}{3};\frac{(i\omega)^2}{4a_1\omega_t^2}\right)\right] + a_1^{-5/6}\frac{1}{(-i\omega)}\left[\frac{(-i\omega)^2}{4a_1\omega_t^2}\right]^{-5/6}\left[\frac{\Gamma\left(\frac{4}{3}\right)}{\Gamma\left(\frac{1}{2}\right)}{}_1F_1\left(-\frac{5}{6};-\frac{1}{3};\frac{(-i\omega)^2}{4a_1\omega_t^2}\right)\right.$$
$$\left.\left. + \frac{\Gamma\left(-\frac{4}{3}\right)}{\Gamma\left(-\frac{5}{6}\right)}\left[\frac{(-i\omega)^2}{4a_1\omega_t^2}\right]^{4/3}{}_1F_1\left(\frac{1}{2};\frac{7}{3};\frac{(-i\omega)^2}{4a_1\omega_t^2}\right)\right]\right\}.$$

After simplifying the expression, we have

$$X = 2(3.87)\hat{\sigma}_R^2\omega_t^{-1}d_3^{-5/6}\,\mathrm{Re}\left\{\left[\frac{\omega}{\omega_t}\right]^{-8/3}\frac{1}{(i)^{8/3}}\left[\frac{\Gamma\left(\frac{4}{3}\right)}{\Gamma\left(\frac{1}{2}\right)}{}_1F_1\left(-\frac{5}{6};-\frac{1}{3};\frac{(i\omega)^2}{4a_1\omega_t^2}\right)\right.\right.$$
$$\left. + \frac{\Gamma\left(-\frac{4}{3}\right)}{\Gamma\left(-\frac{5}{6}\right)}\left[\frac{\omega}{\omega_t}\right]^{8/3}\frac{(i)^{8/3}}{(4a_1)^{4/3}}{}_1F_1\left(\frac{1}{2};\frac{7}{3};\frac{(i\omega)^2}{4a_1\omega_t^2}\right)\right] + \left[\frac{\omega}{\omega_t}\right]^{-8/3}\frac{1}{(-i)^{8/3}}\left[\frac{\Gamma\left(\frac{4}{3}\right)}{\Gamma\left(\frac{1}{2}\right)}{}_1F_1\left(-\frac{5}{6};-\frac{1}{3};\frac{(-i\omega)^2}{4a_1\omega_t^2}\right)\right.$$
$$\left.\left. + \frac{\Gamma\left(-\frac{4}{3}\right)}{\Gamma\left(-\frac{5}{6}\right)}\left[\frac{\omega}{\omega_t}\right]^{8/3}\frac{(-i)^{8/3}}{(4a_1)^{4/3}}{}_1F_1\left(\frac{1}{2};\frac{7}{3};\frac{(-i\omega)^2}{4a_1\omega_t^2}\right)\right]\right\}.$$

Note, the arguments of the ${}_1F_1$ functions can be simplified by observing that $(i)^2 = (-i)^2 = -1$, and by distributing $\left[\frac{\omega}{\omega_t}\right]^{-8/3}$, $\frac{1}{(i)^{8/3}}$, and $\frac{1}{(-i)^{8/3}}$, respectively, and collecting like expressions, we have

$$X = 2(3.87)\hat{\sigma}_R^2 \omega_t^{-1} d_3^{-5/6} \operatorname{Re}\left\{\left[\frac{\omega}{\omega_t}\right]^{-8/3} \frac{\Gamma\left(\frac{4}{3}\right)}{\Gamma\left(\frac{1}{2}\right)} {}_1F_1\left(-\frac{5}{6};-\frac{1}{3};-\frac{\omega^2}{4a_1\omega_t^2}\right)\left[\frac{1}{(i)^{8/3}}+\frac{1}{(-i)^{8/3}}\right]\right.$$
$$\left. + \frac{\Gamma\left(-\frac{4}{3}\right)}{\Gamma\left(-\frac{5}{6}\right)} \frac{2}{(4a_1)^{4/3}} {}_1F_1\left(\frac{1}{2};\frac{7}{3};-\frac{\omega^2}{4a_1\omega_t^2}\right)\right\}.$$

Using (G2), in appendix G, and factoring $\frac{(-1)\Gamma\left(\frac{4}{3}\right)}{\Gamma\left(\frac{1}{2}\right)}$ we have,

$$X = -2(3.87) \frac{\Gamma\left(\frac{4}{3}\right)}{\Gamma\left(\frac{1}{2}\right)} \hat{\sigma}_R^2 \omega_t^{-1} d_3^{-5/6} \operatorname{Re}\left\{\left[\frac{\omega}{\omega_t}\right]^{-8/3} {}_1F_1\left(-\frac{5}{6};-\frac{1}{3};-\frac{\omega^2}{4a_1\omega_t^2}\right)\right.$$
$$\left. - \frac{2\Gamma\left(-\frac{4}{3}\right)\Gamma\left(\frac{1}{2}\right)}{\Gamma\left(-\frac{5}{6}\right)\Gamma\left(\frac{4}{3}\right)} \frac{1}{(4a_1)^{4/3}} {}_1F_1\left(\frac{1}{2};\frac{7}{3};-\frac{\omega^2}{4a_1\omega_t^2}\right)\right\},$$

or equivalently

$$X = -\frac{3.90\hat{\sigma}_R^2}{\omega_t d_3^{5/6}} \operatorname{Re}\left\{\left[\frac{\omega}{\omega_t}\right]^{-8/3} {}_1F_1\left(-\frac{5}{6};-\frac{1}{3};-\frac{\omega^2}{4a_1\omega_t^2}\right) + 0.29\frac{1}{a_1^{4/3}} {}_1F_1\left(\frac{1}{2};\frac{7}{3};-\frac{\omega^2}{4a_1\omega_t^2}\right)\right\}. \qquad \text{E 1}$$

As for evaluating the integral Y, the procedures will be identical to those taken for evaluating integral X. So, let's start by substituting the limit into integral Y, which gives

$$Y = \lim_{\alpha\to 0}\left(2(3.87)\hat{\sigma}_R^2(\Lambda d_3)^{5/6} \operatorname{Re}\left\{\int_0^\infty {}_1F_1\left(-\frac{5}{6};1;-a_2\omega_t^2\tau^2\right)e^{-(\alpha+i\omega)}d\tau + \int_0^\infty {}_1F_1\left(-\frac{5}{6};1;-a_2\omega_t^2\tau^2\right)e^{-(\alpha-i\omega)}d\tau\right\}\right).$$

By writing the hypergeometric functions in their summation form, assuming term-wise integration is permitted, using integral A1 and property A12, in appendix A, we have

$$Y = \lim_{\alpha\to 0}\left(2(3.87)\hat{\sigma}_R^2(\Lambda d_3)^{5/6} \operatorname{Re}\left\{\frac{1}{\alpha+i\omega} {}_2F_0\left(-\frac{5}{6},\frac{1}{2};-\frac{4a_2\omega_t^2}{[\alpha+i\omega]^2}\right) + \frac{1}{\alpha-i\omega} {}_2F_0\left(-\frac{5}{6},\frac{1}{2};-\frac{4a_2\omega_t^2}{[\alpha-i\omega]^2}\right)\right\}\right).$$

After performing the limit operation, we have

$$Y = 2(3.87)\hat{\sigma}_R^2(\Lambda d_3)^{5/6} \operatorname{Re}\left\{\frac{1}{(i\omega)} {}_2F_0\left(-\frac{5}{6},\frac{1}{2};-\frac{4a_2\omega_t^2}{[i\omega]^2}\right) + \frac{1}{(-i\omega)} {}_2F_0\left(-\frac{5}{6},\frac{1}{2};-\frac{4a_2\omega_t^2}{[-i\omega]^2}\right)\right\}.$$

Again, let's transform the hypergeometric function, ${}_2F_0$, into a linear combination of confluent hypergeometric ${}_1F_1$ functions, using (F2), in appendix F, we have

$$Y = 2(3.87)\hat{\sigma}_R^2(\Lambda d_3)^{5/6}\,\mathrm{Re}\left\{\frac{1}{(i\omega)}\left[\frac{(i\omega)^2}{4a_2\omega_t^2}\right]^{-5/6}\left[\frac{\Gamma\left(\frac{4}{3}\right)}{\Gamma\left(\frac{1}{2}\right)}{}_1F_1\left(-\frac{5}{6};-\frac{1}{3};\frac{(i\omega)^2}{4a_2\omega_t^2}\right)\right.\right.$$
$$+\frac{\Gamma\left(-\frac{4}{3}\right)}{\Gamma\left(-\frac{5}{6}\right)}\left[\frac{(\pm i\omega)^2}{4a_2\omega_t^2}\right]^{4/3}{}_1F_1\left(\frac{1}{2};\frac{7}{3};\frac{(i\omega)^2}{4a_2\omega_t^2}\right)\Bigg]+\frac{1}{(-i\omega)}\left[\frac{(-i\omega)^2}{4a_2\omega_t^2}\right]^{-5/6}\left[\frac{\Gamma\left(\frac{4}{3}\right)}{\Gamma\left(\frac{1}{2}\right)}{}_1F_1\left(-\frac{5}{6};-\frac{1}{3};\frac{(-i\omega)^2}{4a_2\omega_t^2}\right)\right.$$
$$\left.\left.+\frac{\Gamma\left(-\frac{4}{3}\right)}{\Gamma\left(-\frac{5}{6}\right)}\left[\frac{(-i\omega)^2}{4a_2\omega_t^2}\right]^{4/3}{}_1F_1\left(\frac{1}{2};\frac{7}{3};\frac{(-i\omega)^2}{4a_2\omega_t^2}\right)\right]\right\}.$$

Recall that $a_2 = \frac{1}{4\Lambda d_3^2}$, which implies that $(a_2)^{5/6} = \frac{1}{(4d_3)^{5/6}(\Lambda d_3)^{5/6}}$ and simplifying the expression, we have

$$Y = 2(3.87)\hat{\sigma}_R^2\omega_t^{-1}d_3^{-5/6}\,\mathrm{Re}\left\{\left[\frac{\omega}{\omega_t}\right]^{-8/3}\frac{1}{(i)^{8/3}}\left[\frac{\Gamma\left(\frac{4}{3}\right)}{\Gamma\left(\frac{1}{2}\right)}{}_1F_1\left(-\frac{5}{6};-\frac{1}{3};\frac{(i\omega)^2}{4a_2\omega_t^2}\right)\right.\right.$$
$$+\frac{\Gamma\left(-\frac{4}{3}\right)}{\Gamma\left(-\frac{5}{6}\right)}\left[\frac{\omega}{\omega_t}\right]^{8/3}\frac{(i)^{8/3}}{(4a_2)^{4/3}}{}_1F_1\left(\frac{1}{2};\frac{7}{3};\frac{(i\omega)^2}{4a_2\omega_t^2}\right)\Bigg]+\left[\frac{\omega}{\omega_t}\right]^{-8/3}\frac{1}{(-i)^{8/3}}\left[\frac{\Gamma\left(\frac{4}{3}\right)}{\Gamma\left(\frac{1}{2}\right)}{}_1F_1\left(-\frac{5}{6};-\frac{1}{3};\frac{(-i\omega)^2}{4a_2\omega_t^2}\right)\right.$$
$$\left.\left.+\frac{\Gamma\left(-\frac{4}{3}\right)}{\Gamma\left(-\frac{5}{6}\right)}\left[\frac{\omega}{\omega_t}\right]^{8/3}\frac{(-i)^{8/3}}{(4a_2)^{4/3}}{}_1F_1\left(\frac{1}{2};\frac{7}{3};\frac{(-i\omega)^2}{4a_2\omega_t^2}\right)\right]\right\}.$$

Again, the arguments of the ${}_1F_1$ functions can be simplified by observing that $(i)^2=(-i)^2=-1$, and by distributing $\left[\frac{\omega}{\omega_t}\right]^{-8/3}$, $\frac{1}{(i)^{8/3}}$, and $\frac{1}{(-i)^{8/3}}$, respectively, using (G2), in appendix G, and factoring $\frac{(-1)\Gamma\left(\frac{4}{3}\right)}{\Gamma\left(\frac{1}{2}\right)}$ we have,

$$Y=-2(3.87)\frac{\Gamma\left(\frac{4}{3}\right)}{\Gamma\left(\frac{1}{2}\right)}\hat{\sigma}_R^2\omega_t^{-1}d_3^{-5/6}\,\mathrm{Re}\left\{\left[\frac{\omega}{\omega_t}\right]^{-8/3}{}_1F_1\left(-\frac{5}{6};-\frac{1}{3};-\frac{\omega^2}{4a_2\omega_t^2}\right)\right.$$
$$\left.-\frac{2\Gamma\left(-\frac{4}{3}\right)\Gamma\left(\frac{1}{2}\right)}{\Gamma\left(-\frac{5}{6}\right)\Gamma\left(\frac{4}{3}\right)}\frac{1}{(4a_2)^{4/3}}{}_1F_1\left(\frac{1}{2};\frac{7}{3};-\frac{\omega^2}{4a_2\omega_t^2}\right)\right\},$$

or equivalently

$$Y=-\frac{3.90\hat{\sigma}_R^2}{\omega_t d_3^{5/6}}\,\mathrm{Re}\left\{\left[\frac{\omega}{\omega_t}\right]^{-8/3}{}_1F_1\left(-\frac{5}{6};-\frac{1}{3};-\frac{\omega^2}{4a_2\omega_t^2}\right)+0.29\frac{1}{a_2^{4/3}}{}_1F_1\left(\frac{1}{2};\frac{7}{3};-\frac{\omega^2}{4a_2\omega_t^2}\right)\right\}. \quad \text{E 2}$$

Since $S_I(\omega)=X-Y$, then by combining (E1) and (E2) it follows that

$$S_{I,l}(\omega)=-\frac{3.90\hat{\sigma}_R^2}{\omega_t d_3^{5/6}}\,\mathrm{Re}\left\{\left[\frac{\omega}{\omega_t}\right]^{-8/3}{}_1F_1\left(-\frac{5}{6};-\frac{1}{3};-\frac{\omega^2}{4a_1\omega_t^2}\right)+0.29\frac{1}{a_1^{4/3}}{}_1F_1\left(\frac{1}{2};\frac{7}{3};-\frac{\omega^2}{4a_1\omega_t^2}\right)\right\}$$
$$+\frac{3.90\hat{\sigma}_R^2}{\omega_t d_3^{5/6}}\,\mathrm{Re}\left\{\left[\frac{\omega}{\omega_t}\right]^{-8/3}{}_1F_1\left(-\frac{5}{6};-\frac{1}{3};-\frac{\omega^2}{4a_2\omega_t^2}\right)+0.29\frac{1}{a_2^{4/3}}{}_1F_1\left(\frac{1}{2};\frac{7}{3};-\frac{\omega^2}{4a_2\omega_t^2}\right)\right\}.$$

Finally, we have

$$S_{I,l}(\omega)=\frac{3.90\hat{\sigma}_R^2}{\omega_t d_3^{5/6}}\operatorname{Re}\left\{\left[\frac{\omega}{\omega_t}\right]^{-8/3}\left[{}_1F_1\left(-\frac{5}{6};-\frac{1}{3};-\frac{\omega^2}{4a_2\omega_t^2}\right)-{}_1F_1\left(-\frac{5}{6};-\frac{1}{3};-\frac{\omega^2}{4a_1\omega_t^2}\right)\right]\right.$$
$$\left.+0.29\left[\frac{1}{a_2^{4/3}}{}_1F_1\left(\frac{1}{2};\frac{7}{3};-\frac{\omega^2}{4a_2\omega_t^2}\right)-\frac{1}{a_1^{4/3}}{}_1F_1\left(\frac{1}{2};\frac{7}{3};-\frac{\omega^2}{4a_1\omega_t^2}\right)\right]\right\}. \qquad \text{E 3}$$

Let's evaluate the radial component of the covariance function, $S_{I,r}(\omega)$, so we have

$$S_{I,r}(\omega)=4(6.45)\hat{\sigma}_R^2(\Lambda d_3)^{5/6}\left(\frac{r^2}{W^2}\right)\int_0^\infty {}_1F_1\left(\frac{1}{6};1;-\frac{\omega_t^2\tau^2}{4\Lambda d_3^2}\right)\cos(\omega\tau)d\tau$$

Again, substitute the limiting case of $\cos(\omega\tau)=\frac{1}{2}\left(e^{i\omega\tau}+e^{-i\omega\tau}\right)=\frac{1}{2}\lim_{\alpha\to 0}\left(e^{-(\alpha+i\omega)\tau}+e^{-(\alpha-i\omega)\tau}\right)$ in the integral gives

$$S_{I,r}(\omega)=\lim_{\alpha\to 0}\left(2(6.45)\hat{\sigma}_R^2(\Lambda d_3)^{5/6}\left(\frac{r^2}{W^2}\right)\operatorname{Re}\left\{\int_0^\infty {}_1F_1\left(\frac{1}{6};1;-\frac{\omega_t^2\tau^2}{4\Lambda d_3^2}\right)e^{-(\alpha+i\omega)}d\tau\right.\right.$$
$$\left.\left.+\int_0^\infty {}_1F_1\left(\frac{1}{6};1;-\frac{\omega_t^2\tau^2}{4\Lambda d_3^2}\right)e^{-(\alpha-i\omega)}d\tau\right\}\right)$$

By writing the hypergeometric functions in their summation form, assuming term-wise integration is permitted, and using integral A1 and property A12, in appendix A, we have

$$S_{I,r}(\omega)=\lim_{\alpha\to 0}\left(2(6.45)\hat{\sigma}_R^2(\Lambda d_3)^{5/6}\left(\frac{r^2}{W^2}\right)\operatorname{Re}\left\{\frac{1}{\alpha-i\omega}{}_2F_0\left(\frac{1}{6},\frac{1}{2};-;-\frac{\omega_t^2}{\Lambda d_3^2(\alpha-i\omega)^2}\right)\right.\right.$$
$$\left.\left.+\frac{1}{\alpha+i\omega}{}_2F_0\left(\frac{1}{6},\frac{1}{2};-;-\frac{\omega_t^2}{\Lambda d_3^2(\alpha+i\omega)^2}\right)\right\}\right).$$

After performing the limit operation, we have

$$S_{I,r}(\omega)=2(6.45)\hat{\sigma}_R^2(\Lambda d_3)^{5/6}\left(\frac{r^2}{W^2}\right)\mathrm{Re}\left\{\frac{1}{(-i\omega)^2}{}_2F_0\left(\frac{1}{6},\frac{1}{2};-;-\frac{\omega_t^2}{\Lambda d_3^2(-i\omega)^2}\right)\right.$$
$$\left.+\frac{1}{(i\omega)^2}{}_2F_0\left(\frac{1}{6},\frac{1}{2};-;-\frac{\omega_t^2}{\Lambda d_3^2(i\omega)^2}\right)\right\}.$$

Let's transform the hypergeometric function, ${}_2F_0$, into a linear combination of confluent hypergeometric ${}_1F_1$ functions by using (F3), in appendix F, we have

$$S_{I,r}(\omega)=2(6.45)\hat{\sigma}_R^2(\Lambda d_3)^{5/6}\left(\frac{r^2}{W^2}\right)\mathrm{Re}\left\{\frac{1}{(-i\omega)}\frac{\Gamma\left(\frac{1}{3}\right)}{\Gamma\left(\frac{1}{2}\right)}\left[\frac{\Lambda d_3^2(-i\omega)^2}{\omega_t^2}\right]^{1/6}\right.$$
$$\times\left[{}_1F_1\left(\frac{1}{6};\frac{2}{3};\frac{\Lambda d_3^2(-i\omega)^2}{\omega_t^2}\right)+\frac{\Gamma\left(-\frac{1}{3}\right)\Gamma\left(\frac{1}{2}\right)}{\Gamma\left(\frac{1}{6}\right)\Gamma\left(\frac{1}{3}\right)}\left[\frac{\Lambda d_3^2(-i\omega)^2}{\omega_t^2}\right]^{1/3}{}_1F_1\left(\frac{1}{2};\frac{4}{3};\frac{\Lambda d_3^2(-i\omega)^2}{\omega_t^2}\right)\right]$$
$$\left.+\frac{1}{(i\omega)}\frac{\Gamma\left(\frac{1}{3}\right)}{\Gamma\left(\frac{1}{2}\right)}\left[\frac{\Lambda d_3^2(i\omega)^2}{\omega_t^2}\right]^{1/6}\left[{}_1F_1\left(\frac{1}{6};\frac{2}{3};\frac{\Lambda d_3^2(i\omega)^2}{\omega_t^2}\right)+\frac{\Gamma\left(-\frac{1}{3}\right)\Gamma\left(\frac{1}{2}\right)}{\Gamma\left(\frac{1}{6}\right)\Gamma\left(\frac{1}{3}\right)}\left[\frac{\Lambda d_3^2(i\omega)^2}{\omega_t^2}\right]^{1/3}{}_1F_1\left(\frac{1}{2};\frac{4}{3};\frac{\Lambda d_3^2(i\omega)^2}{\omega_t^2}\right)\right]\right\}.$$

After simplifying the expression, we have

$$S_{I,r}(\omega)=2(6.45)\hat{\sigma}_R^2(\Lambda d_3)^{5/6}\left(\frac{r^2}{W^2}\right)\frac{\Gamma\left(\frac{1}{3}\right)}{\Gamma\left(\frac{1}{2}\right)}\frac{\left(\Lambda d_3^2\right)^{1/6}}{\omega_t}\left(\frac{\omega}{\omega_t}\right)^{-2/3}\left\{{}_1F_1\left(\frac{1}{6};\frac{2}{3};-\frac{\Lambda d_3^2\omega^2}{\omega_t^2}\right)\right.$$

$$\left.\times\left[\frac{1}{(-i)^{2/3}}-\frac{1}{i^{2/3}}\right]+2\frac{\Gamma\left(-\frac{1}{3}\right)\Gamma\left(\frac{1}{2}\right)}{\Gamma\left(\frac{1}{6}\right)\Gamma\left(\frac{1}{3}\right)}\left(\Lambda d_3^2\right)^{1/3}\left(\frac{\omega}{\omega_t}\right)^{2/3}{}_1F_1\left(\frac{1}{2};\frac{4}{3};-\frac{\Lambda d_3^2\omega^2}{\omega_t^2}\right)\right\}.$$

Finally, using (G3), in appendix G, and further simplifying, we have

$$S_{I,r}(\omega)=2(6.45)\frac{\Gamma\left(\frac{1}{3}\right)}{\Gamma\left(\frac{1}{2}\right)}\hat{\sigma}_R^2\frac{\Lambda d_3^{7/6}}{\omega_t}\left(\frac{r^2}{W^2}\right)\left(\frac{\omega}{\omega_t}\right)^{-2/3}\left\{{}_1F_1\left(\frac{1}{6};\frac{2}{3};-\frac{\Lambda d_3^2\omega^2}{\omega_t^2}\right)\right.$$

$$\left.+2\frac{\Gamma\left(-\frac{1}{3}\right)\Gamma\left(\frac{1}{2}\right)}{\Gamma\left(\frac{1}{6}\right)\Gamma\left(\frac{1}{3}\right)}\left(\Lambda d_3^2\right)^{1/3}\left(\frac{\omega}{\omega_t}\right)^{2/3}{}_1F_1\left(\frac{1}{2};\frac{4}{3};-\frac{\Lambda d_3^2\omega^2}{\omega_t^2}\right)\right\},$$

or equivalently

$$S_{I,r}(\omega)=19.4924\hat{\sigma}_R^2\frac{\Lambda d_3^{7/6}}{\omega_t}\left(\frac{r^2}{W^2}\right)\left(\frac{\omega}{\omega_t}\right)^{-2/3}\left\{{}_1F_1\left(\frac{1}{6};\frac{2}{3};-\frac{\Lambda d_3^2\omega^2}{\omega_t^2}\right)\right.$$

$$\left.-0.965722\left(\Lambda d_3^2\right)^{1/3}\left(\frac{\omega}{\omega_t}\right)^{2/3}{}_1F_1\left(\frac{1}{2};\frac{4}{3};-\frac{\Lambda d_3^2\omega^2}{\omega_t^2}\right)\right\}. \qquad \text{E 4}$$

APPENDIX F: APPLICATION OF THE MEIJER G-FUNCTION

Lets transform the hypergeometric ${}_2F_0(a,b;-;z)$ function into a Meijer G-function, using property A8, in appendix A, we see that $p=2,\ q=0,\ m=2,\ n=1,\ a_1=a,\ a_2=b.$ So we have,

$${}_2F_0(a,b;-;z)=\frac{\prod_{j=1}^{0}\Gamma(c_j)}{\prod_{j=1}^{2}\Gamma(a_j)}G_{1,2}^{2,1}\left[-\frac{1}{z}\middle|\begin{matrix}1\\ a,\quad b\end{matrix}\right]=\frac{1}{\Gamma(a)\Gamma(b)}G_{1,2}^{2,1}\left[-\frac{1}{z}\middle|\begin{matrix}1\\ a,\quad b\end{matrix}\right].$$

Let's transform $G_{1,2}^{2,1}\left[-\frac{1}{z}\middle|\begin{matrix}1\\ a,\quad b\end{matrix}\right]$ into the form ${}_pF_q$ by using property A6, in appendix A. For $G_{1,2}^{2,1}\left[-\frac{1}{z}\middle|\begin{matrix}1\\ a,\quad b\end{matrix}\right]$, we see that $m=2,\ n=1,\ p=1,$ and $q=2,$ which leads to

$$G_{1,2}^{2,1}\left[-\frac{1}{z}\middle|\begin{matrix}1\\ a,\quad b\end{matrix}\right]=\frac{\Gamma(a-b)\Gamma(1+a-1)}{(1)(1)}\left[-\frac{1}{z}\right]^{a}{}_1F_1\left(1+a-1;1+a-b;(-1)^{1-2-1}\left(-\frac{1}{z}\right)\right)$$
$$+\frac{\Gamma(a-b)\Gamma(1+b-1)}{(1)(1)}\left[-\frac{1}{z}\right]^{b}{}_1F_1\left(1+b-1;1+b-a;(-1)^{1-2-1}\left(-\frac{1}{z}\right)\right).$$

By multiplying both sides by $\frac{1}{\Gamma(a)\Gamma(b)}$, we have

$$\frac{1}{\Gamma(a)\Gamma(b)}G_{1,2}^{2,1}\left[-\frac{1}{z}\middle|\begin{matrix}1\\ a,\quad b\end{matrix}\right]=\frac{\Gamma(b-a)}{\Gamma(b)}\left[-\frac{1}{z}\right]^{a}{}_1F_1\left(a;1+a-b;-\frac{1}{z}\right)+\frac{\Gamma(a-b)}{\Gamma(a)}\left[-\frac{1}{z}\right]^{b}{}_1F_1\left(b;1+b-a;-\frac{1}{z}\right).$$

It follows that

$${}_2F_0(a,b;-;z)=\frac{\Gamma(b-a)}{\Gamma(b)}\left[-\frac{1}{z}\right]^{a}{}_1F_1\left(a;1+a-b;-\frac{1}{z}\right)+\frac{\Gamma(a-b)}{\Gamma(a)}\left[-\frac{1}{z}\right]^{b}{}_1F_1\left(b;1+b-a;-\frac{1}{z}\right).\quad \text{F 1}$$

Let's transform the hypergeometric ${}_2F_0\left(-\frac{5}{6},\frac{1}{2};-;-\frac{4b\omega_t^2}{(\pm i\omega)}\right)$ using (F1). We see that $a=-\frac{5}{6}$,

$b=\frac{1}{2}$, and $z=-\frac{4b\omega_t^2}{(\pm i\omega)^2}$ which implies that $-\frac{1}{z}=\frac{(\pm i\omega)^2}{4b\omega_t^2}$. It follows that

$$
{}_2F_0\left(-\frac{5}{6},\frac{1}{2};-;-\frac{4b\omega_t^2}{(\pm i\omega)^2}\right)=\frac{\Gamma\left(\frac{4}{3}\right)}{\Gamma\left(\frac{1}{2}\right)}\left[\frac{(\pm i\omega)^2}{4b\omega_t^2}\right]^{-5/6}{}_1F_1\left(-\frac{5}{6};-\frac{1}{3};\frac{(\pm i\omega)^2}{4b\omega_t^2}\right)
$$
$$
+\frac{\Gamma\left(-\frac{4}{3}\right)}{\Gamma\left(-\frac{5}{6}\right)}\left[\frac{(\pm i\omega)^2}{4b\omega_t^2}\right]^{1/2}{}_1F_1\left(\frac{1}{2};\frac{7}{3};\frac{(\pm i\omega)^2}{4b\omega_t^2}\right).
$$

By factoring $\frac{\Gamma\left(\frac{4}{3}\right)}{\Gamma\left(\frac{1}{2}\right)}\left[\frac{(\pm i\omega)^2}{4b\omega_t^2}\right]^{-5/6}$, then

$$
{}_2F_0\left(-\frac{5}{6},\frac{1}{2};-;-\frac{4b\omega_t^2}{(\pm i\omega)^2}\right)=\frac{\Gamma\left(\frac{4}{3}\right)}{\Gamma\left(\frac{1}{2}\right)}\left[\frac{(\pm i\omega)^2}{4b\omega_t^2}\right]^{-5/6}\left\{{}_1F_1\left(-\frac{5}{6};-\frac{1}{3};\frac{(\pm i\omega)^2}{4b\omega_t^2}\right)\right.
$$
$$
\left.+\frac{\Gamma\left(-\frac{4}{3}\right)\Gamma\left(\frac{1}{2}\right)}{\Gamma\left(-\frac{5}{6}\right)\Gamma\left(\frac{4}{3}\right)}\left[\frac{(\pm i\omega)^2}{4b\omega_t^2}\right]^{4/3}{}_1F_1\left(\frac{1}{2};\frac{7}{3};\frac{(\pm i\omega)^2}{4b\omega_t^2}\right)\right\}. \qquad \text{F 2}
$$

Now let's transform the hypergeometric ${}_2F_0\left(\frac{1}{6},\frac{1}{2};-;-\frac{4b\omega_t^2}{(\pm i\omega)}\right)$ using (F1), we see that $a=\frac{1}{6}$,

$b=\frac{1}{2}$, and $z=-\frac{4b\omega_t^2}{(\pm i\omega)^2}$ which implies that $-\frac{1}{z}=\frac{(\pm i\omega)^2}{4b\omega_t^2}$. It follows that

$$ {}_2F_0\left(\frac{1}{6},\frac{1}{2};-;-\frac{4b\omega_t^2}{(\pm i\omega)^2}\right)=\frac{\Gamma\left(\frac{1}{3}\right)}{\Gamma\left(\frac{1}{2}\right)}\left[\frac{(\pm i\omega)^2}{4b\omega_t^2}\right]^{1/6}{}_1F_1\left(\frac{1}{6};\frac{2}{3};\frac{(\pm i\omega)^2}{4b\omega_t^2}\right) $$

$$ +\frac{\Gamma\left(-\frac{1}{3}\right)}{\Gamma\left(\frac{1}{6}\right)}\left[\frac{(\pm i\omega)^2}{4b\omega_t^2}\right]^{1/2}{}_1F_1\left(\frac{1}{2};\frac{4}{3};\frac{(\pm i\omega)^2}{4b\omega_t^2}\right). $$

By factoring $\frac{\Gamma\left(\frac{1}{3}\right)}{\Gamma\left(\frac{1}{2}\right)}\left[\frac{(\pm i\omega)^2}{4b\omega_t^2}\right]^{1/6}$, then

$$ {}_2F_0\left(\frac{1}{6},\frac{1}{2};-;-\frac{4b\omega_t^2}{(\pm i\omega)^2}\right)=\frac{\Gamma\left(\frac{1}{3}\right)}{\Gamma\left(\frac{1}{2}\right)}\left[\frac{(\pm i\omega)^2}{4b\omega_t^2}\right]^{1/6}\left\{{}_1F_1\left(\frac{1}{6};\frac{2}{3};\frac{(\pm i\omega)^2}{4b\omega_t^2}\right)\right. $$

$$ \left.+\frac{\Gamma\left(-\frac{1}{3}\right)\Gamma\left(\frac{1}{2}\right)}{\Gamma\left(\frac{1}{6}\right)\Gamma\left(\frac{1}{3}\right)}\left[\frac{(\pm i\omega)^2}{4b\omega_t^2}\right]^{1/3}{}_1F_1\left(\frac{1}{2};\frac{4}{3};\frac{(\pm i\omega)^2}{4b\omega_t^2}\right)\right\}. \qquad \text{F 3} $$

APPENDIX G: ADDITIONAL PROPERTIES

From complex variables, we know the following properties for complex expressions:

A. $x \pm iy = re^{\pm i\vartheta}$, where $r = \sqrt{x^2 + y^2}$ and $\vartheta = \tan^{-1}\left(\frac{y}{x}\right)$

B. $e^{i\vartheta} = \cos\vartheta + i\sin\vartheta$

C. $\mathrm{Re}\{e^{i\vartheta}\} = \cos\vartheta$ and $\mathrm{Im}\{e^{i\vartheta}\} = \sin\vartheta$

D. $\left(e^{i\vartheta}\right)^n = \cos(n\vartheta) + i\sin(n\vartheta)$

Let's consider the following complex expressions. First, consider the complex expression $\left[1 - \frac{i\left(1 - \overline{\Theta} d_3\right)}{\Lambda d_3}\right]^{\alpha}$, where α is a rational. Let's begin by rewriting the complex expression as

$$\left[1 - \frac{i\left(1 - \overline{\Theta} d_3\right)}{\Lambda d_3}\right]^{\alpha} = \left(\Lambda d_3\right)^{-\alpha}\left[\left(\Lambda d_3\right) - i\left(1 - \overline{\Theta} d_3\right)\right]^{\alpha} = \left(\Lambda d_3\right)^{-\alpha}\left[\left(\Lambda d_3\right)^2 + \left(1 - \overline{\Theta} d_3\right)^2\right]^{\alpha/2} \exp\left[i(-\alpha)\tan^{-1}\left(\frac{1 - \overline{\Theta} d_3}{\Lambda d_3}\right)\right].$$

Thus the real component of the complex expression is given as

$$\mathrm{Re}\left\{\left[1 - \frac{i\left(1 - \overline{\Theta} d_3\right)}{\Lambda d_3}\right]^{\alpha}\right\} = \left(\Lambda d_3\right)^{-\alpha}\left[\left(\Lambda d_3\right)^2 + \left(1 - \overline{\Theta} d_3\right)^2\right]^{\alpha/2} \cos\left[(-\alpha)\tan^{-1}\left(\frac{1 - \overline{\Theta} d_3}{\Lambda d_3}\right)\right]$$

$$= \left(\Lambda d_3\right)^{-\alpha}\left[\left(\Lambda d_3\right)^2 + \left(1 - \overline{\Theta} d_3\right)^2\right]^{\alpha/2} \cos\left[\alpha \tan^{-1}\left(\frac{1 - \overline{\Theta} d_3}{\Lambda d_3}\right)\right]. \qquad \text{G 1}$$

Next, let's simplify the complex expression $\frac{1}{(i)^{8/3}} + \frac{1}{(-i)^{8/3}}$. Since $i = e^{i\pi/2}$, then it follows that $(i)^{8/3} = e^{i4\pi/3}$ and $(i)^{-8/3} = e^{-i4\pi/3}$. Similarly, since $-i = e^{-i\pi/2}$, it follows that $(-i)^{8/3} = e^{-i4\pi/3}$ and $(-i)^{-8/3} = e^{i4\pi/3}$. So we have

$$\frac{1}{(i)^{8/3}}+\frac{1}{(-i)^{8/3}}=e^{-i4\pi/3}+e^{i4\pi/3}=2\cos\left(\frac{4\pi}{3}\right)=2\left(-\frac{1}{2}\right)=-1. \qquad \text{G 2}$$

Finally, let's simplify the complex expression $\frac{1}{(-i)^{2/3}}+\frac{1}{(i)^{2/3}}$. Since $i=e^{i\pi/2}$, then it follows that $(i)^{2/3}=e^{i\pi/3}$ and $(i)^{-2/3}=e^{-i\pi/3}$. Similarly, since $-i=e^{-i\pi/2}$, it follows that $(-i)^{2/3}=e^{-i\pi/3}$ and $(-i)^{-2/3}=e^{i\pi/3}$. So we have

$$\frac{1}{(-i)^{2/3}}+\frac{1}{(i)^{2/3}}=e^{i\pi/3}+e^{-i\pi/3}=2\cos\left(\frac{\pi}{3}\right)=2\left(\frac{1}{2}\right)=1. \qquad \text{G 3}$$

APPENDIX H: QUASI-FREQUENCY

The quasi-frequency for the longitudinal component of the covariance function of irradiance fluctuations is given as

$$\nu_0 = \frac{1}{2\pi}\left[\frac{B_{I,l}''(0,L)}{B_{I,l}(0,L)}\right]^{1/2}. \qquad \text{H 1}$$

From appendix D, we have the longitudinal component of the covariance function under the weak turbulence theory and frozen turbulence hypothesis given as (D2)

$$B_{I,l}(\tau,L) = 8\pi^2 k^2 L \int_0^1\int_0^\infty \kappa\Phi_n(\kappa)\exp\left(-\frac{\Lambda L\xi^2\kappa^2}{k}\right)\mathrm{Re}\left\{J_0\left[\kappa V_\perp \tau\right]\left(1-\exp\left[-\frac{iL\kappa^2}{k}\xi\left(1-\overline{\Theta}\xi\right)\right]\right)\right\}d\kappa d\xi .$$

Using the thin phase screen model to evaluate (D2) leads to (D9)

$$B_{I,l}(\tau,L) = 3.8637\hat{\sigma}_R^2\,\mathrm{Re}\left\{i^{5/6}\left[1-\left(\overline{\Theta}+i\Lambda\right)d_3\right]^{5/6}{}_1F_1\left(-\frac{5}{6};1;-a_1\omega_\perp^2\tau^2\right)-\left(\Lambda d_3\right)^{5/6}{}_1F_1\left(-\frac{5}{6};1;-a_2\omega_t^2\tau^2\right)\right\},$$

where $d_3 = 0.67 - 0.17\Theta$, $a_1 = \dfrac{1}{4d_3 i\left[1-\left(\overline{\Theta}+i\Lambda\right)d_3\right]}$, and $a_2 = \dfrac{1}{4\Lambda d_3^2}$. Taking $\tau = 0$, then (D9) simplifies to

$$B_{I,l}(0,L) = 3.8637\hat{\sigma}_R^2\,\mathrm{Re}\left\{i^{5/6}\left[1-\left(\overline{\Theta}+i\Lambda\right)d_3\right]^{5/6}-\left(\Lambda d_3\right)^{5/6}\right\},$$

and finding the real component leads to

$$B_{I,l}(0,L) = 3.8637\hat{\sigma}_R^2\left\{\left[\left(\Lambda d_3\right)^2+\left(1-\overline{\Theta}d_3\right)^2\right]^{5/12}\cos\left[\frac{5}{6}\tan^{-1}\left(\frac{1-\overline{\Theta}d_3}{\Lambda d_3}\right)\right]-\left(\Lambda d_3\right)^{5/6}\right\}. \qquad \text{H 2}$$

Assuming uniform convergence and differentiating (D2) twice with respect to τ, we have

$$B'_{I,l}(\tau,L)=8\pi^2k^2L\int_0^1\int_0^\infty \kappa\Phi_n(\kappa)\exp\left(-\frac{\Lambda L\xi^2\kappa^2}{k}\right)\mathrm{Re}\left\{-(\kappa V_\perp)J_1(\kappa V_\perp\tau)\right.$$
$$\left.+\exp\left[-\frac{iL\kappa^2}{k}\xi\left(1-\overline{\Theta}\xi\right)\right](\kappa V_\perp)J_1(\kappa V_\perp\tau)\right\}d\kappa d\tau, \qquad \text{H 3}$$

and

$$B''_{I,l}(\tau,L)=-8\pi^2k^2L\int_0^1\int_0^\infty \kappa\Phi_n(\kappa)\exp\left(-\frac{\Lambda L\xi^2\kappa^2}{k}\right)\mathrm{Re}\left\{(\kappa V_\perp)^2\left[J_0(\kappa V_\perp\tau)\right.\right.$$
$$\left.-\frac{1}{\kappa V_\perp\tau}J_1(\kappa V_\perp\tau)\right]+\exp\left[-\frac{iL\kappa^2}{k}\xi\left(1-\overline{\Theta}\xi\right)\right](\kappa V_\perp)^2\left[J_0(\kappa V_\perp\tau)-\frac{1}{\kappa V_\perp\tau}J_1(\kappa V_\perp\tau)\right]\Bigg\}d\kappa d\tau. \qquad \text{H 4}$$

Let's use the thin phase screen model and take $d_2 << 1$ which implies that $1+d_2\eta\cong 1$ where $0\le\eta\le 1$. In addition, let's set $\tau=0$, then (H4) becomes

$$B''_{I,l}(0,L)=-4\pi^2k^2V_\perp^2Ld_2d_3\int_0^\infty \kappa^3\Phi_n(\kappa)\exp\left(-\frac{\Lambda Ld_3^2}{k}\kappa^2\right)d\kappa$$
$$+4\pi^2k^2V_\perp^2Ld_2d_3\,\mathrm{Re}\left\{\int_0^\infty \kappa^3\Phi_n(\kappa)\exp\left(-\frac{\Lambda Ld_3^2}{k}\kappa^2\right)\exp\left[-\frac{iLd_3}{k}\left(1-\overline{\Theta}d_3\right)\kappa^2\right]d\kappa\right\}. \qquad \text{H 5}$$

Separating (H5) into two integrals, let

$$A=-4\pi^2k^2V_\perp^2Ld_2d_3\int_0^\infty \kappa^3\Phi_n(\kappa)\exp\left(-\frac{\Lambda Ld_3^2}{k}\kappa^2\right)d\kappa$$

and

$$B = 4\pi^2 k^2 V_\perp^2 L d_2 d_3 \,\mathrm{Re}\left\{\int_0^\infty \kappa^3 \Phi_n(\kappa) \exp\left(-\frac{\Lambda L d_3^2}{k}\kappa^2\right) \exp\left[-\frac{iLd_3}{k}\left(1-\overline{\Theta} d_3\right)\kappa^2\right] d\kappa\right\}.$$

Let's use the Kolmogorov spectrum $\Phi_n(\kappa) = (0.033)\hat{C}_n^2 \kappa^{-11/3}$, where $\hat{C}_n^2$ is the refractive-index structure constant of the phase screen, to evaluate the integrals A and B. Starting the integral A, we have

$$A = -4(0.033)\pi^2 \hat{C}_n^2 k^2 V_\perp^2 L d_2 d_3 \int_0^\infty \kappa^{-2/3} \exp\left(-\frac{\Lambda L d_3^2}{k}\kappa^2\right) d\kappa.$$

Let's make a change of variable of integration and set $x = \kappa^2$, which will lead to

$$A = -2(0.033)\pi^2 \hat{C}_n^2 k^2 V_\perp^2 L d_2 d_3 \int_0^\infty x^{-5/6} \exp\left(-\frac{\Lambda L d_3^2}{k} x\right) dx.$$

Using integral A1 from appendix A, we have

$$A = -2(0.033)\pi^2 \hat{C}_n^2 k^2 V_\perp^2 L d_2 d_3 \Gamma\left(\frac{1}{6}\right)\left(\frac{k}{\Lambda L d_3^2}\right)^{1/6}. \qquad \text{H 6}$$

Then for integral B, we have

$$B = 4(0.033)\pi^2 \hat{C}_n^2 k^2 V_\perp^2 L d_2 d_3 \,\mathrm{Re}\left\{\int_0^\infty \kappa^{-2/3} \exp\left[-\kappa^2 \frac{Ld_3}{k}\left(\Lambda d_3 + i\left(1-\overline{\Theta} d_3\right)\right)\right] d\kappa\right\}.$$

Again, making a change of variable of integration and setting $x = \kappa^2$ leads to

$$B = 2(0.033)\pi^2 \hat{C}_n^2 k^2 V_\perp^2 L d_2 d_3 \,\mathrm{Re}\left\{\int_0^\infty x^{-5/6} \exp\left[-x\frac{L d_3}{k}\left(\Lambda d_3 + i\left(1-\overline{\Theta} d_3\right)\right)\right] dx\right\}.$$

Using integral A1 from appendix A, we have

$$B = 2(0.033)\pi^2 \hat{C}_n^2 k^2 V_\perp^2 L d_2 d_3 \,\mathrm{Re}\left\{\Gamma\left(\frac{1}{6}\right)\left(\frac{k}{L d_3}\right)^{1/6}\left(\Lambda d_3 + i\left(1-\overline{\Theta} d_3\right)\right)^{-1/6}\right\}.$$

Finding the real component leads to

$$B = 2(0.033)\Gamma\left(\frac{1}{6}\right)\pi^2 \hat{C}_n^2 V_\perp^2 k^{13/6} L^{5/6} d_2 d_3 \left\{\left(\Lambda d_3\right)^2 + \left(1-\overline{\Theta} d_3\right)^2 \cos\left[\frac{1}{6}\tan^{-1}\left(\frac{1-\overline{\Theta} d_3}{\Lambda d_3}\right)\right]\right\}. \quad \text{H 7}$$

Combining the results of (H6) and (H7), then simplifying leads to

$$B''_{I,l}(0,L) = 2\left(0.033\right)\Gamma\left(\frac{1}{6}\right)\pi^2\, \hat{C}_n^2\, V_\perp^2\, k^{13/6}\, L^{5/6}\, d_2\, d_3^{5/6}\left\{\left(\Lambda d_3\right)^2 + \left(1-\overline{\Theta}\, d_3\right)^2 \cos\left[\frac{1}{6}\tan^{-1}\left(\frac{1-\overline{\Theta} d_3}{\Lambda d_3}\right)\right] - \left(\Lambda d_3\right)^{-1/6}\right\}. \quad \text{H 8}$$

Using (H2) and (H8), the quasi-frequency defined by (H1) becomes

$$\nu_0 = \frac{1}{2\pi}\left[-\frac{5V_\perp^2 k\left\{\Lambda^{1/6} d_3^{1/6}\left[\left(\Lambda d_3\right)^2 + \left(1-\overline{\Theta} d_3\right)^2\right]^{-1/12}\cos\left[\frac{1}{6}\tan^{-1}\left(\frac{1-\overline{\Theta} d_3}{\Lambda d_3}\right)\right] - 1\right\}}{12 L d_3^{7/6}\Lambda^{1/6}\left[\left(\Lambda d_3\right)^2 + \left(1-\overline{\Theta} d_3\right)^2\right]^{5/12}\cos\left[\frac{5}{6}\tan^{-1}\left(\frac{1-\overline{\Theta} d_3}{\Lambda d_3}\right)\right] - \Lambda d_3^{5/6}}\right]^{1/2}. \quad \text{H 9}$$

The quasi-frequency expressed by (H9) is not valid for plane and spherical waves, where $\Lambda = 0$, thus (H9) is valid for collimated beams.

REFERENCES

1. **Richardson, L. F.** *Weather Prediction By Numerical Process.* Cambridge : University Press, 1922.

2. **Young, Hugh D.** *University Physics.* 8th. New York : Addison-Wesley, 1992.

3. *Comparison between the extended-medium and the phase screen scintillation theories.* **Booker, H. G., Ferguson, J.A. and Vats, H.O.** 1985, Atmos. Terres. Physics, Vol. 47, pp. 381-399.

4. *Propagation of a Gaussian-beam wave through a Random Phase Screen.* **Andrews, Larry C, Phillips, Ron L and Weeks, A. R.** 1997, Wave Random Media, Vol. 7, pp. 229-244.

5. **Andrews, Larry C and Phillips, Ron L.** *Laser Beam Propagation Through Random Media.* 2nd. Bellingham, Washington : SPIE Press, 2005.

6. *Statistical Properties Of A Sine Wave Plus Random Noise.* **Rice, S. O.** 1948, Bell Sys. Tech., Vol. 27, pp. 109-158.

7. *The Mathematical Analysis Of Random Noise.* **Rice, S. O.** 1944, Bell Sys. Tech., Vol. 23, pp. 282-332.

8. —. **Rice, S. O.** 1945, Bell Sys. Tech., Vol. 24, pp. 46-156.

9. **Andrews, Larry C.** *Special Functions Of Mathematics For Engineers.* 2nd. Bellingham, Washington : SPIE Press, 1998.